A Newtonian Model for Spiral Galaxy Rotation Curves

Geoffrey M. Williams
email : gmwill@charter.net

Abstract

A spiral galaxy is modeled as a thin, flat, axisymmetric disk comprising a series of concentric, coplanar rings. Using conventional Newtonian gravitation kinematics, it is shown that relatively flat velocity curves are produced by a variety of possible mass distributions in the disk. No halo of "dark matter" is needed to produce these rotation curves. Compared with a point mass at the center, the disk gravitational force grows with increasing distance from the disk center, crests and then slowly subsides beyond the disk perimeter. The model is applied to the NGC 3198, M31 and NGC 4736 galaxies, with ring masses adjusted to match the respective velocity profiles. Gravitational force fields in the disk are calculated, leading to direct estimates of enclosed galaxy mass. The mass distributions of several other spiral galaxies are analyzed, and their basic characteristics are charted in Appendix 2.

Subject headings: galaxies: kinematics and dynamics-gravitation-mass distribution

Introduction

Spiral galaxies are disks containing billions of stars and matter, rotating about the disk center. This mass of material is held together by gravitational forces counteracting the centrifugal forces of disk rotation. When astronomers started reviewing the rotation curves of spiral galaxies, they were surprised to find, that as distance from the disk center increased, circular velocities did not decline.

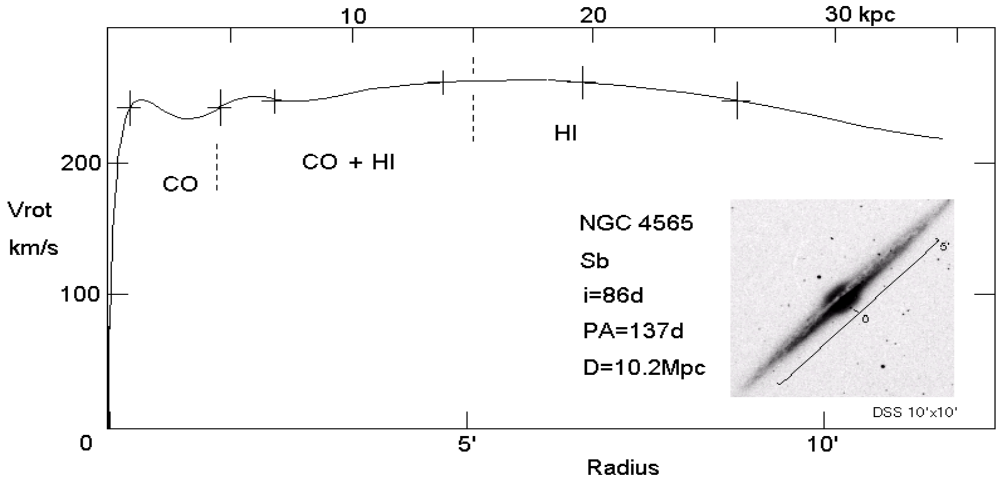

Figure 1. Rotation Curve for Spiral Galaxy NGC 4565 (Reference 1)

A typical example of the radial profile of circular velocity of a spiral galaxy is shown in Figure 1. After the initial rise from the disk center, the circular velocity remains essentially constant (or flat). This velocity profile contrasts with that of the solar system, where the orbital velocity of the outer planets about the sun, is markedly slower than that of the inner planets. Various hypotheses have been developed to explain the unexpected galaxy rotation curves. This paper seeks to demonstrate that the gravitational field in the disk plane, is modified in a way which leads to the observed rotation curves of spiral galaxies. The distribution of mass throughout the disk, and the thin, flat disk are the key features which modify the gravitational field. For star systems with a *spherically symmetric* mass distribution, there is a theorem by Newton (Reference 2, p.34) stating that the gravitational force at a given radius is determined solely by the mass *inward* from that radius. The images of spiral galaxies show them to be disks of visible star mass that are clearly *not* spherically symmetric distributions, so the theorem is inapplicable. The model developed in this paper shows that the gravitational force in the disk plane at any radius, must recognize the mass both *inward* and *outward* from that radius.

To construct a model for numerical analysis of the galactic disk, the basic element is a *ring* of matter. Later, the *disk* will be modeled by a series of concentric, coplanar ring elements.

Gravitational Force in the Ring Plane

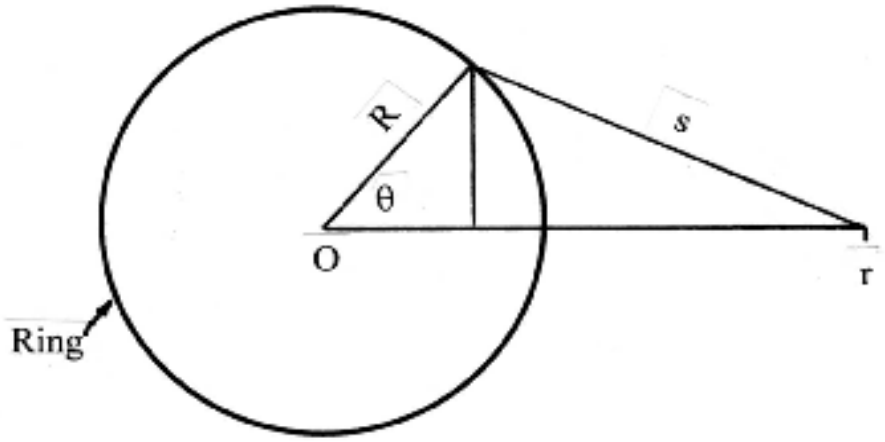

Figure 2. Force Diagram in Ring Plane

If F(r) is the gravitational force in the plane of a ring element of mass ΔM, then

$$F(r) = \frac{G\,\Delta M}{2\pi}\int_0^{2\pi}\left[\frac{r-R\cos\theta}{s^3}\right]d\theta \qquad (1)$$

$$F(r) = \frac{G\,\Delta M}{r^2}\,H(\zeta) \quad \text{where } \zeta = \frac{R}{r} \qquad (2)$$

$$H(\zeta) = \frac{1}{2\pi} \int_0^{2\pi} \left[\frac{(1 - \zeta \cos\theta)}{(1 + \zeta^2 - 2\zeta\cos\theta)^{3/2}} \right] d\theta \qquad (3)$$

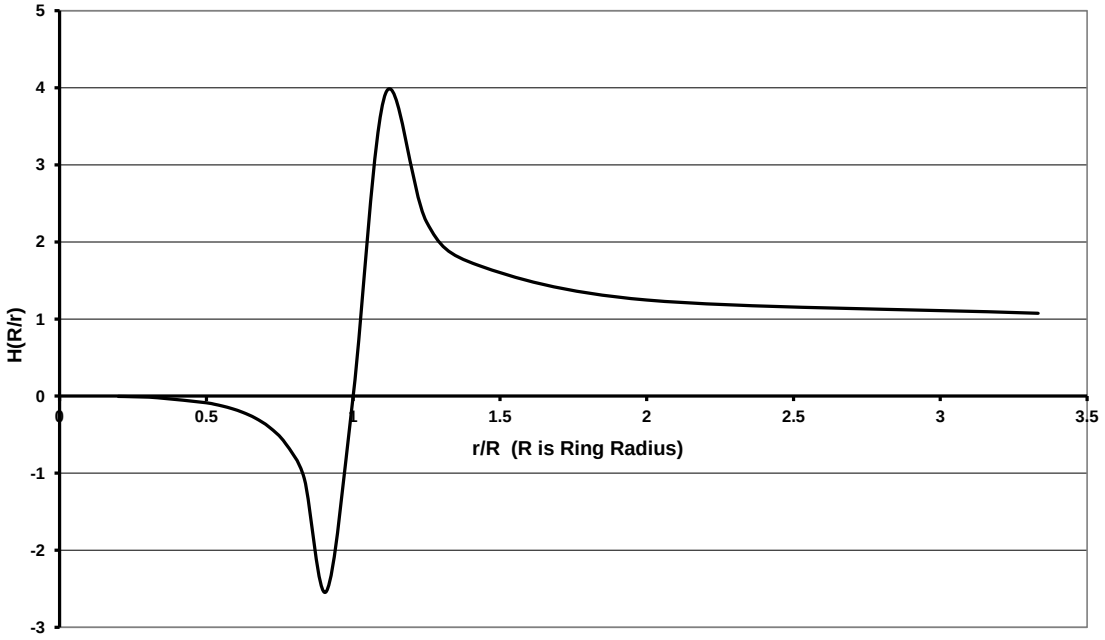

Figure 3. H(R/r) in Ring Plane

The function H(R/r) can be integrated numerically to give the result shown in Figure 3. *Beyond* the ring, the force is positive (attracting toward the ring center). It peaks and then subsides, so that from about r/R = 2, the force will start to match the characteristics of a point mass at the ring center. *Within* the ring, the force is negative (attracting toward the ring, but *away* from the center). There is a negative peak near the ring and then the force subsides to zero at the ring center. (A fuller derivation is provided in Reference 3.)

Gravitational Forces in the Disk Plane

A model of a thin, axially symmetric disk is constructed with a series of n concentric, coplanar rings. The basic model comprises a series of 10 equally-spaced rings at r/R_m = 0.05, 0.15, 0.25,…etc…0.85,0.95. The numerical integration proceeds with summation steps at r/R_m = 0.1, 0.2, 0.3….etc…0.9, 1.0 and further, as desired . Here R_m denotes the edge or "rim" radius of the disk selected for evaluation. Each ring is allotted its respective fraction of the total mass of the disk within R_m, in accordance with an assumed mass distribution.

The gravitational force in the disk plane and toward the disk center, at radius (r_i/R_m) is given by

$$F(r_i/R_m) = \frac{1}{(r_i/R_m)^2} \sum_{i=1}^{n} \Delta M_i \; [\, H(R_m/r_i)] \qquad (4)$$

To demonstrate the model, a radial profile of mass distribution in the disk is chosen as a linear variation, such that the slope of the line is -80 percent. This is noted as an "L80" mass distribution and is illustrated in Figure 4.

(Various mass distributions, both linear and non-linear, have been tested to review their effect on the radial velocity profile of the model. Appendix 1 of this paper describes how a specific mass distribution can be derived, which matches the observed rotation curve for a given spiral galaxy.)

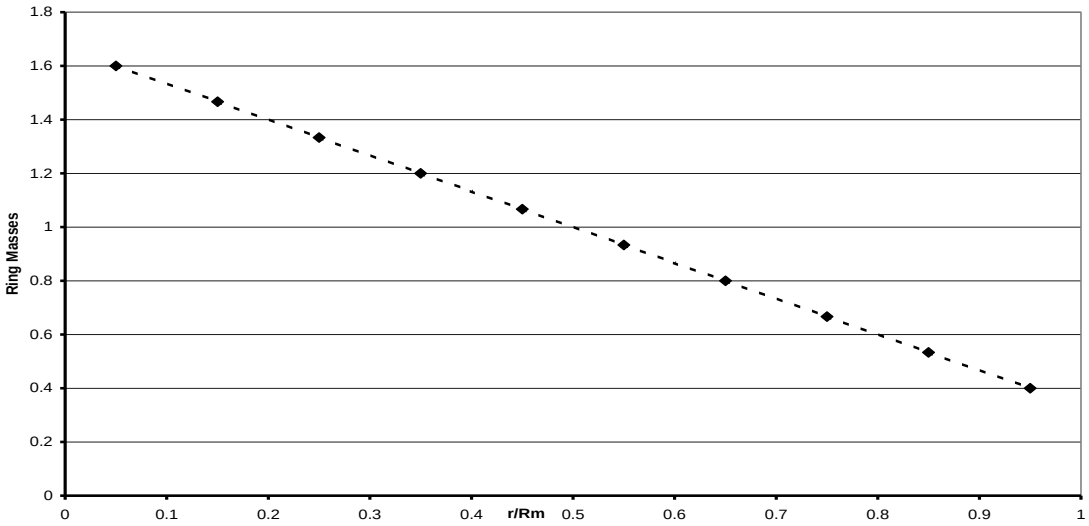

Figure 4. Ring Masses for L80 Mass Distribution

The area of the disk increases with the radius, so the surface mass density at the disk center is several hundred times the value at the disk rim, as illustrated in Figure 5.

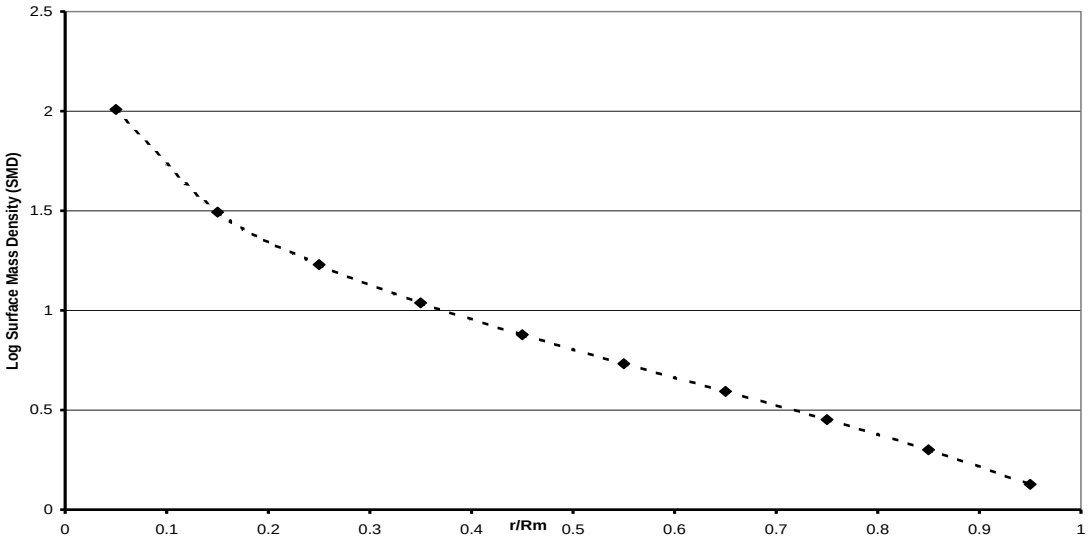

Figure 5. Surface Mass Density for L80 Mass Distribution

The calculated gravitational force in the plane of the disk is shown in Figure 6.

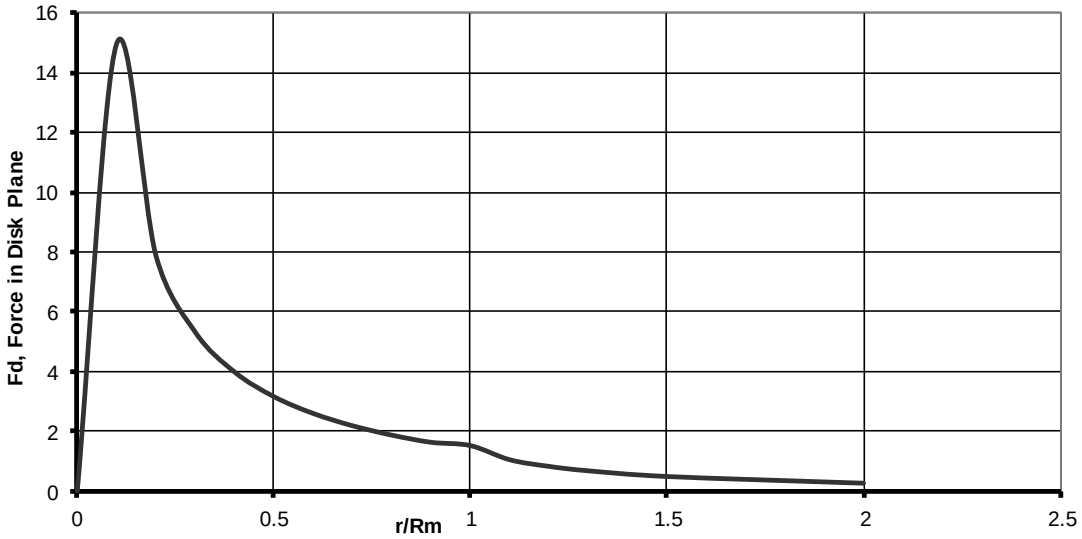

Figure 6. Gravitational Force in Disk Plane for L80 Mass Distribution

Comparing the disk force (F_d) to the force from a point mass (F_p) located at the disk center, is more instructive, as illustrated in Figure 7.

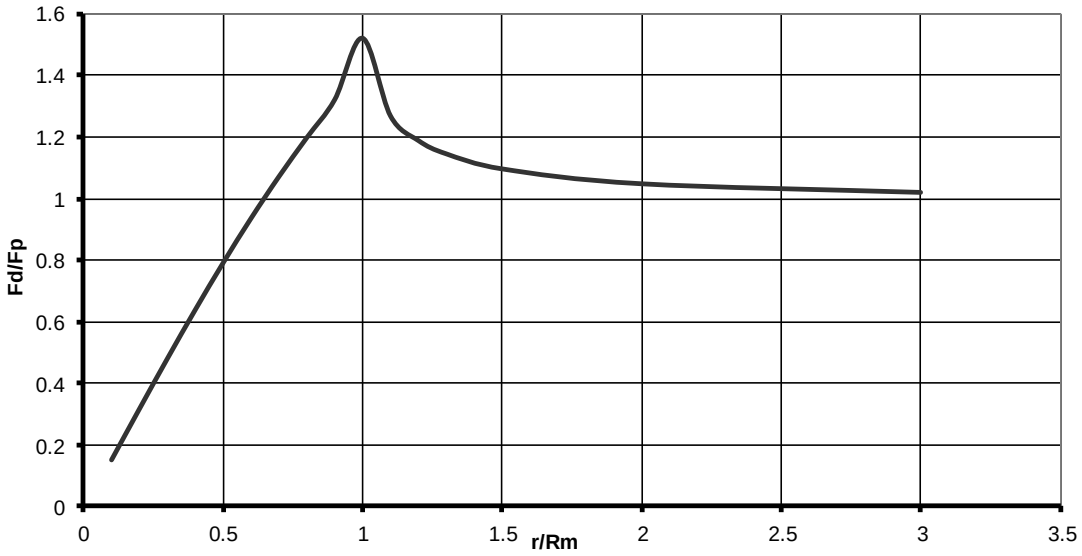

Figure 7. Disk Force vs. Force for Point Mass (L80 Mass Distribution)

For the L80 mass distribution, the disk force factor (F_d/F_p) increases from the disk center, passes through unity at about r/R_m=0.7, and crests to a value of about 1.5 at the disk rim. (The

factor (F_d/F_p) peaks nearer the disk center for rotation curves that decline substantially before R_m). The enhancement of the gravitational force in the disk plane subsides only gradually beyond R_m. From about $r/R_m = 2$, the ratio (F_d/F_p) approaches unity, and the gravitational force then proceeds as a Keplerian decline.

Circular Velocities in the Disk

The circular velocity V_i at radius $\{r_i/R_m\}$ is given by

$$V_i^2 = \{F(r_i/R_m)\}\{r_i/R_m\} \qquad (5)$$

Balancing the centrifugal and gravitational forces at any radius produces the rotation curve shown in Figure 8. This relatively flat profile corresponds to the observed velocity profiles for many spiral galaxies. Note that in the normalized rotation curve for the L80 mass distribution, the circular velocity at $r/R_m = 1$ is $V_m^* = 1.24$

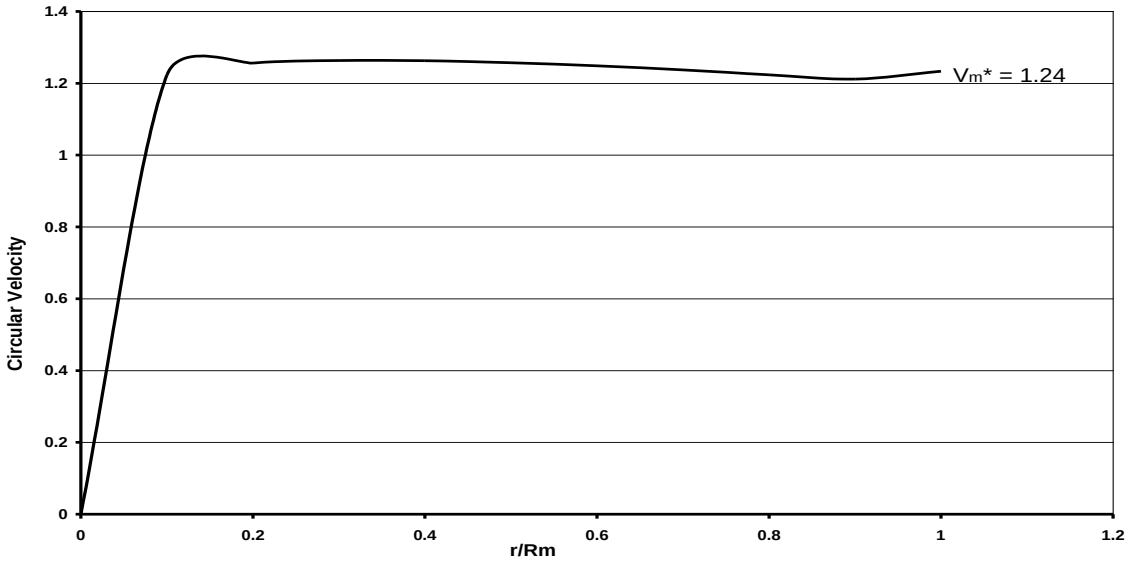

Figure 8. Rotation Curve for L80 Mass Distribution

Estimation of the Mass of a Spiral Galaxy

The total disk galaxy mass includes both the optically observable star matter and the (radio-observable) gas clouds, out to the farthest measured data point. With this simple model, no attempt is made to take specific account of features such as the nuclear bulge, possible black hole, etc. at the center of a typical spiral galaxy. However, with the presumption that the rotation curve is solely dependent on the mass distribution in the disk, the derived mass distribution may nevertheless have given some recognition to these other features.

The enclosed galaxy mass within the radial limit of R_m, is given by

$$M_{R_m} = \frac{(R_m \, x \, V_m^2)}{\{G \; x \; (F_d/F_p)_m\}} \qquad (6)$$

For equation 6 to be valid, R_m must be located at the *outermost* radial point of velocity data measurement (and where disk mass density has effectively declined to zero). The gravitational constant for the purposes of this paper is given by

$$G \approx 4.3 \; x \; 10^{-6} \text{ kpc } (\text{km/s})^2 \; M_{\odot}^{-1}$$

Using a "trial and error" adjustment of the model ring masses has proven capable of achieving a reasonable match with real spiral galaxy velocity profiles. Two examples (NGC 3198 and M31, Andromeda) are provided below. (A detailed description of the convergence method used to determine the individual ring masses that produce a rotation curve matching a given spiral galaxy (NGC 4736), is provided in Appendix 1 of this paper.)

Model for NGC 3198

The rotation curve for NGC 3198 (as taken from Reference 2, p.601) is shown in Figure 9.

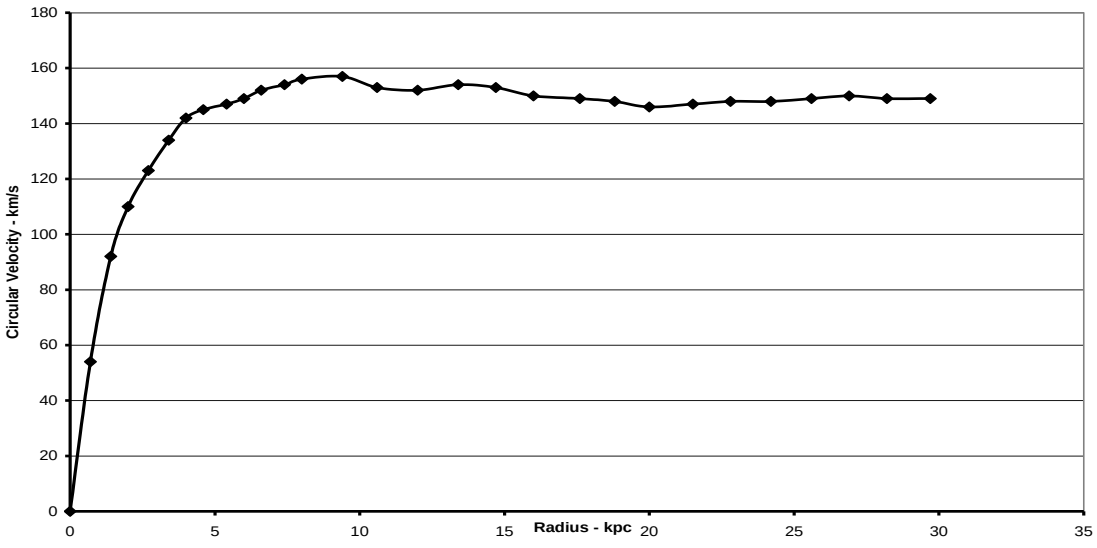

Figure 9. Radial Profile of Circular Velocity for NGC 3198

The basic Model which utilized 10 rings, has been increased to 12 rings, which gives improved modeling capability near the disk center. The matching of the velocity curves for NGC 3198 and the Model is shown in Figure 10.

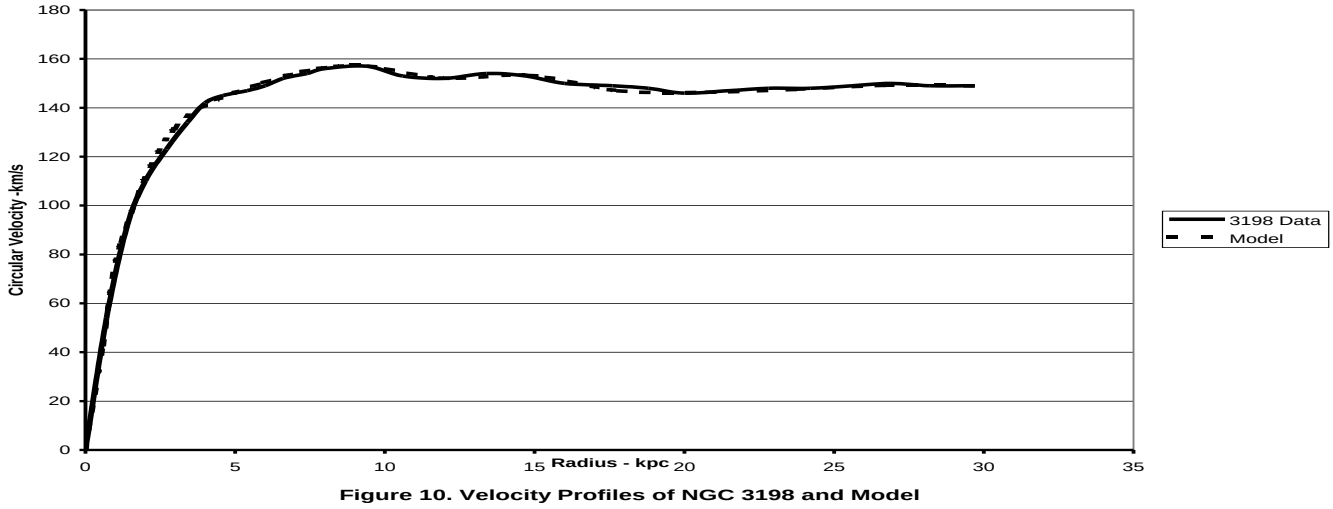

Figure 10. Velocity Profiles of NGC 3198 and Model

The relevant data for estimation of enclosed galaxy mass within R_m are:

R_m = 29.7 kpc V_m = 149 km/s $(F_d/F_p)_m$ = 1.527

Mass of NGC 3198 is….. $M_m = 10.04 \times 10^{10} M_\odot$

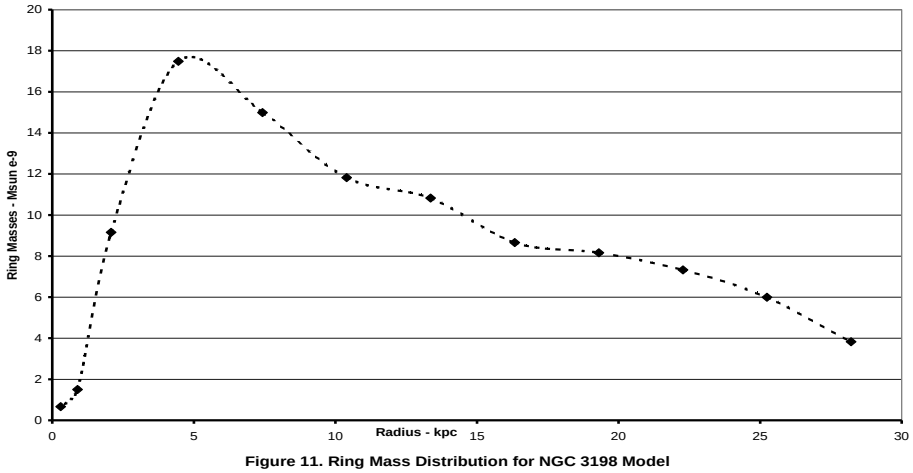

Figure 11. Ring Mass Distribution for NGC 3198 Model

Figure 11 gives the ring mass distribution that produced the model velocity profile (shown as the dashed line in Figure 10) .

Figure 12 translates the ring mass distribution of Figure 11 into a Surface Mass Density format. Figure 13 illustrates the buildup of enclosed galaxy mass for the NGC 3198 Model.

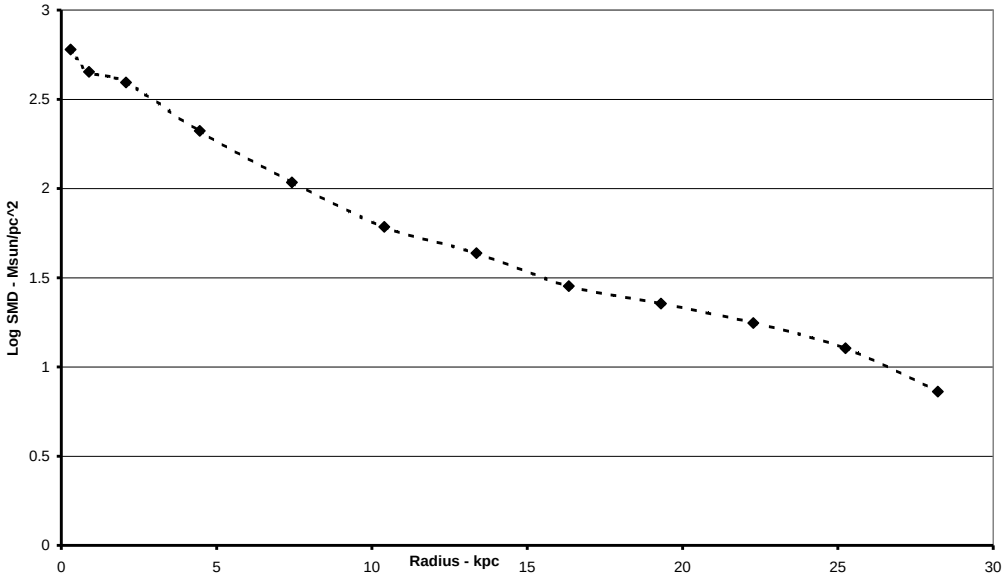

Figure 12. Surface Mass Density for NGC 3198 Model

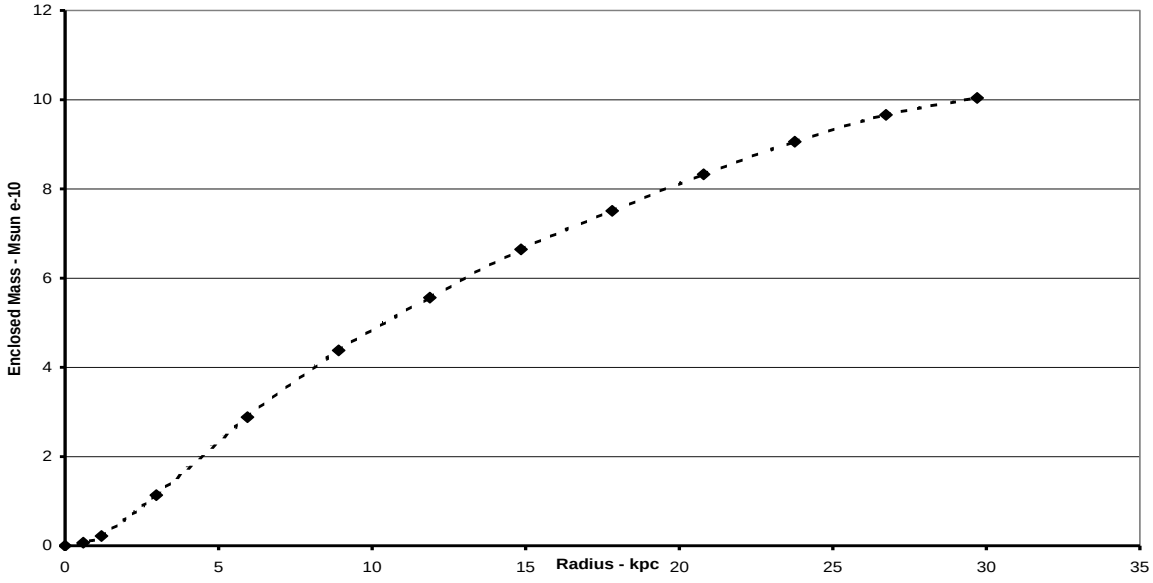

Figure 13. Enclosed Mass for NGC 3198 Model

Model for M31 (Andromeda Galaxy)

The rotation curve values for M31 (as taken from Reference 4.) are shown in Figure 14.

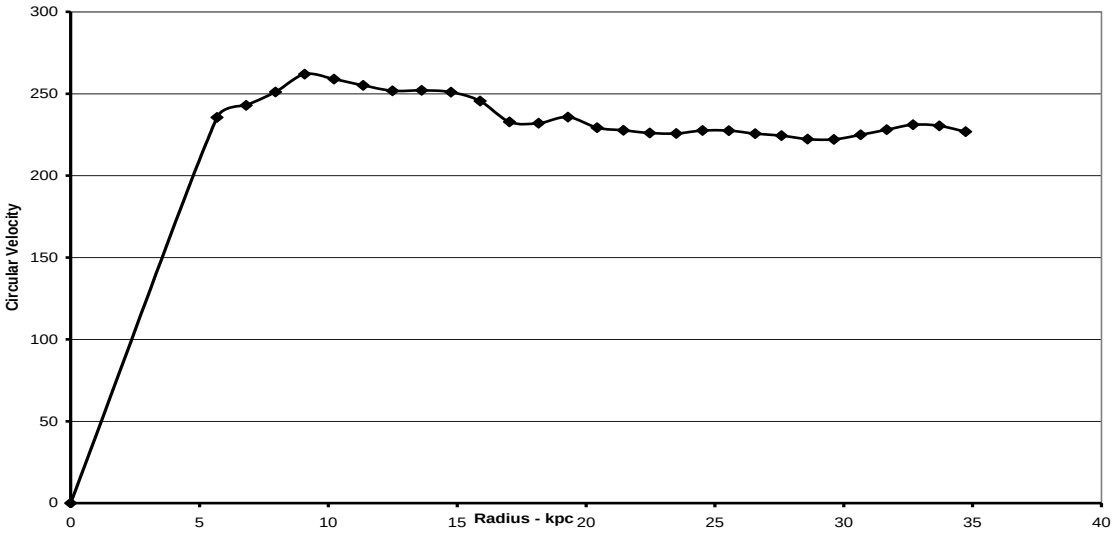

Figure 14. Radial Profile of Circular Velocity for M31

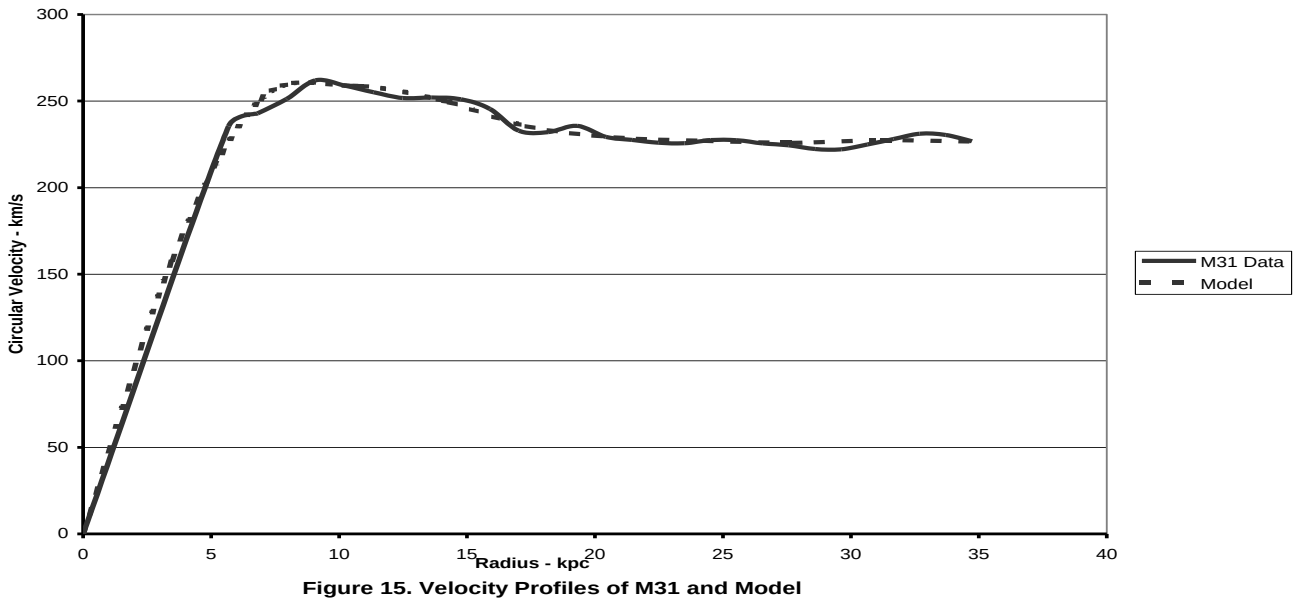

Figure 15. Velocity Profiles of M31 and Model

Figure 15 shows the Model achieving a reasonable match with the rotation curve of M31.

The relevant data for estimating the galaxy mass of M31 enclosed within R_m are:

$R_m = 34.73$ kpc $\qquad V_m = 226.8$ km/s $\qquad (Fd/Fp)_m = 1.485$

Mass of M31 is…. $\qquad M_m = 28.0 \times 10^{10} M_\odot$

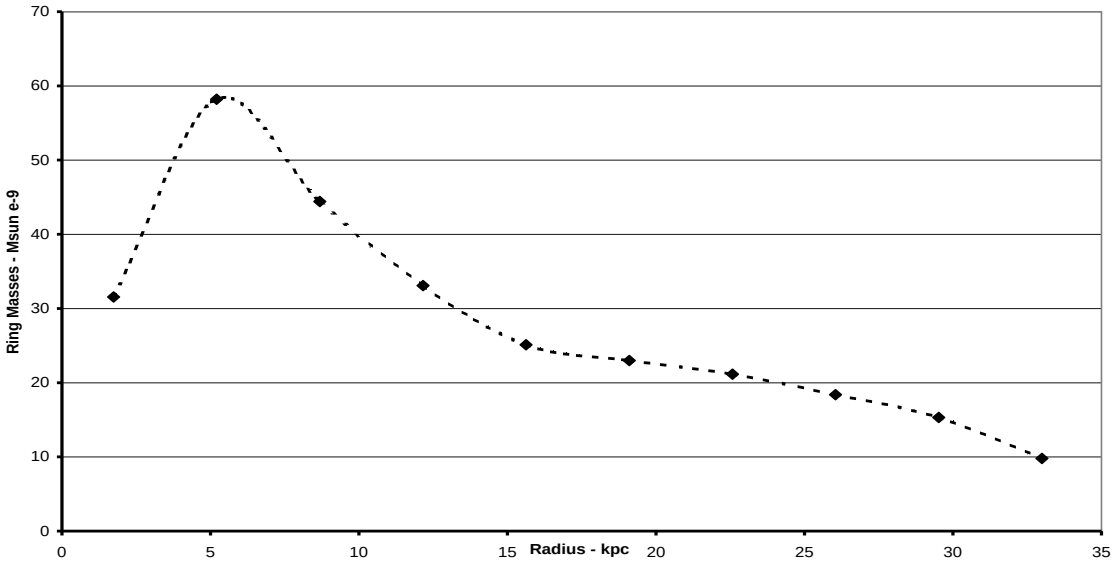

Figure 16. Ring Mass Distribution for M31 Model

Figure 16 shows the ring mass distribution that produced the model velocity profile (shown as the dashed line in Figure 15). Figure 17 translates the ring mass distribution of Figure 16 into a Surface Mass Density format. Figure 18 illustrates the buildup of Enclosed Galaxy Mass for the M31 Model.

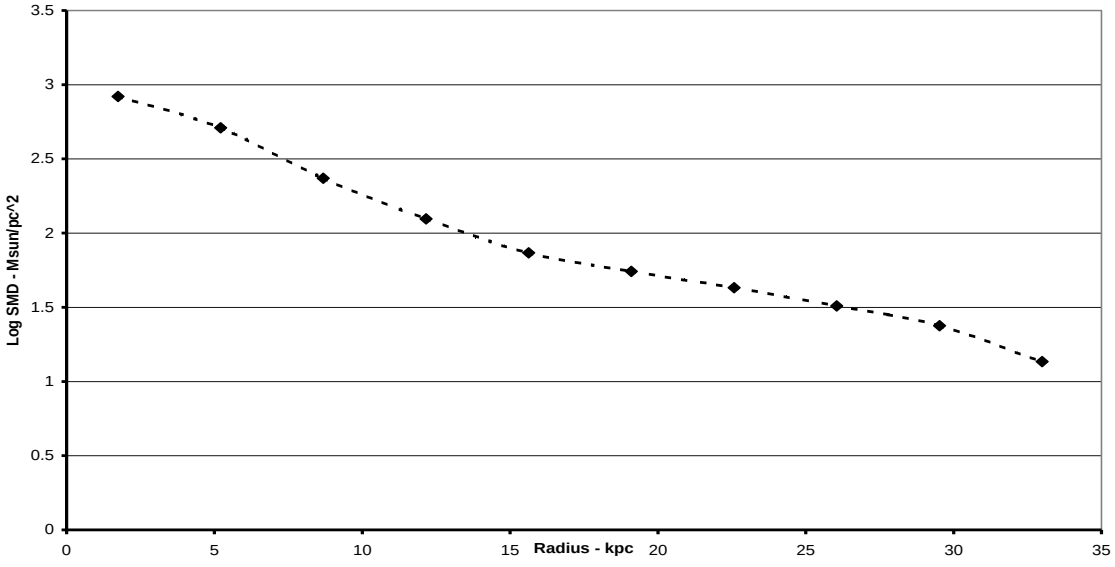

Figure 17. Surface Mass Density for M31 Model

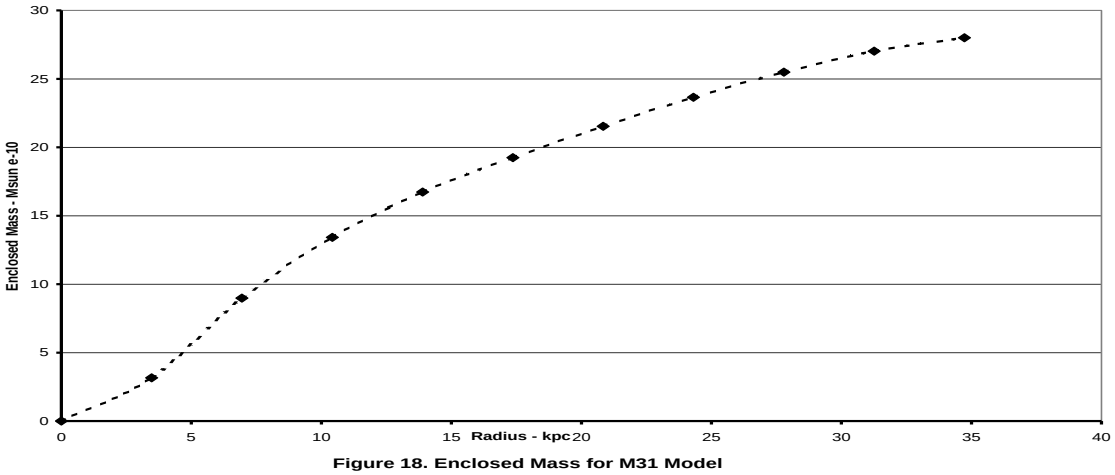

Figure 18. Enclosed Mass for M31 Model

Discussion

Dark Matter Models

The "traditional" method of estimating the mass distribution in spiral galaxies has been to decompose the galaxy into its various features such as disk, gas, dark matter halo, etc. as indicated in Figure 19.

.

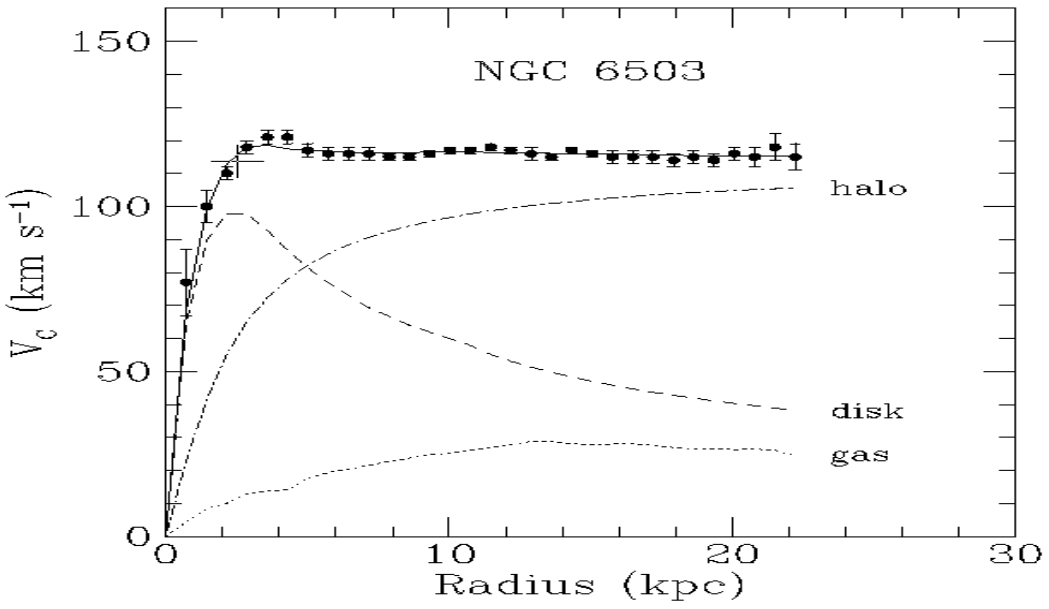

Figure 19. Typical Mass Components of (traditional) Galaxy Model

Allowing the various components to separately satisfy certain assumptions (such as mass-luminosity relationships) produced estimates of individual component mass and its radial

distribution. When these contributions were summed, it became apparent that there was insufficient observable component mass to produce the flat rotation curve. The halo of dark matter was introduced to make up for this apparent deficiency in observable mass in the outer region of the spiral galaxy model. The proportion of dark matter mass to estimated total galaxy mass could be as high as 50 percent (or more) in these traditional studies.

Newtonian Model

In contrast to the techniques and assumptions adopted in the traditional studies, the proposed Newtonian model exclusively uses the observed rotation curves to derive the radial profiles of mass distribution in the disk. There have been a number of other models (a list is provided in Reference 7.) that also are based exclusively on the observed rotation curves of spiral galaxies. These models do not utilize the measured light distribution, and so have no need to make assumptions about the possible coupling of mass surface density and the measured surface brightness profile.

Spiral Galaxies have substantial thickness in their disks, as is apparent in any edge-on images. So the thin, flattened disk model (of 10 or 12 rings) proposed in this paper may be considered simplistic. However, various approximations are utilized in measuring the rotation curve data for any given spiral galaxy, so the current model is probably adequate for predicting the enclosed galaxy mass and the mass distribution in the disk. Appendix 2 provides summary details of several spiral galaxies that have been analyzed using the Newtonian model proposed in this paper. Table 1 of Appendix 2 shows that the force factor $(F_d/F_p)_m$ and the average surface mass density (SMD_{av}) vary over a considerable range, depending on the rotation curve of the individual spiral galaxy.

The predictions of galaxy mass distribution may provide an approach to validating the model. The force field above and below the galaxy disk (within a spherical volume extending to a radius of say, R_m) should be anisotropic, in conformity with the predicted surface mass density profile of the disk. This may be confirmable by examining the orbits of such tracer objects as globular clusters, planetary nebulae, etc.

Acknowledgments

The author gratefully acknowledges the many insights and direction provided him by the listed references.

References

1. *Rotation Curves of Spiral Galaxies* Sofue, Y. and Rubin,V.
2001, Ann. Rev. Astron. Astrophys. 39,137
http://www.ioa.s.u-tokyo.ac.jp/~sofue/h-rot.htm

2. *Galactic Dynamics* Binney, J. and Tremain, S. 1987
Princeton University Press

3. *Gravitational Force in a Thin Disk of Matter* Thayer Watkins,
San Jose State University, California
http://www.applet-magic.com/gravdisk.htm

4. *Extended HI Rotation Curve and Mass Distribution of M31*
Claude Carignan, Laurent Chemin, Walter K. Huchtmeier, and
Felix J. Lockman 6 Mar 2006
arXiv:astro-ph/0603143v1

5. *Is dark matter present in NGC 4736? An iterative spectral method of finding mass distribution in spiral galaxies* Joanna Jalocha, Lukasz Bratek, Marek Kutschera
The Henryk Niewodniczanski Institute of Nuclear Physics, Polish Academy of Science, Poland. 30 Jan 2008
arXiv:astro-ph/0611113v3

6. *The Extended Rotation Curve and the Dark Matter Halo of M33*
Edvige Corbelli, Paolo Salucci, Sep 1999
arXiv:astro-ph/9909252v1

7. *Galactic Rotation Described with Various Thin-Disk Gravitational Models*
James Q. Feng and C.F. Gallo, 1 April 2008
arXiv:0804.0217v1 [astro-ph.GA]

8. *The mass distribution in early type disk galaxies*
Edo Noordermeer, Thijs van der Hulst, Oct 2003
arXiv:astro-ph/0310868v1

9. *HI Study of the NGC 6744 System*
Stuart D. Ryder, Wilfred Walsh and David Malin
Publ. Astron. Soc. Aust., 1999, 16, 84-8

10. *The published extended rotation curves of spiral galaxies: etc.*
R.H. Sanders 1996
arXiv:astro-ph/9606089v1

11. *Galaxy Rotation Curves without Non-Baryonic Dark Matter*
J.R. Brownstein and J.W. Moffat, Sep 2005
arXiv:astro-ph/0506370v4

12. *General Relativity Resolves Galactic Rotation without Exotic Dark Matter*
F.I. Cooperstock and S.Tieu, Jul 2005
arXiv:astro-ph/0507619v1

13. *Spiral Galaxy Rotation Curves determined from Carmelian General Relativity*
John G. Hartnett, Feb 2008
arXiv:astro-ph/0511756v3

Appendix 1.

This Appendix describes the convergent method used to derive the discrete ring mass distribution that produces a model velocity profile that satisfactorily matches the rotation curve for a given spiral galaxy. The rotation curve for NGC 4736 (from Reference 5) is used to demonstrate the method and is illustrated in Figure 20.

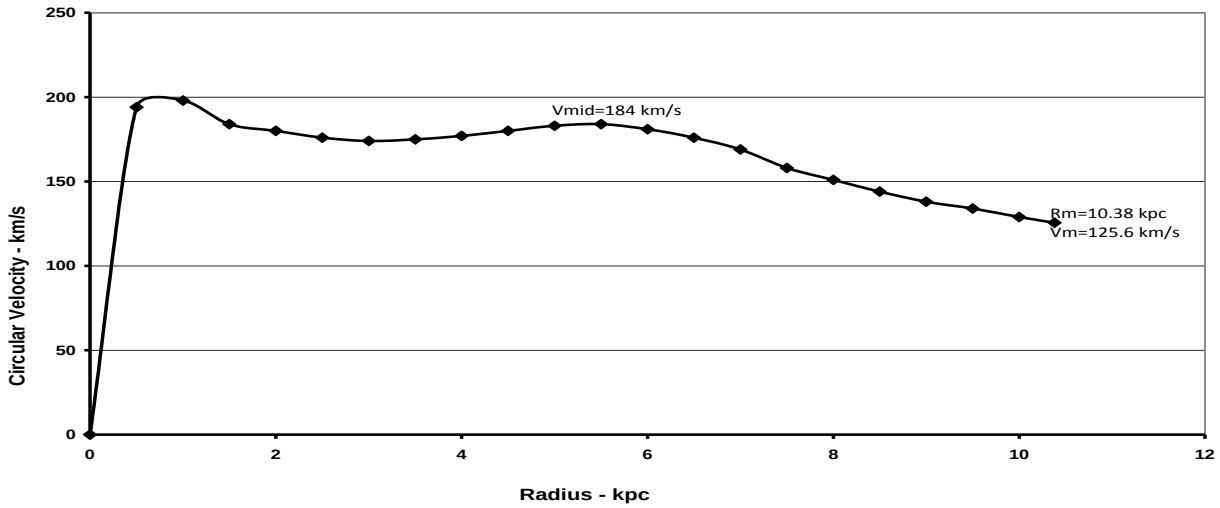

Figure 20. Radial Profile of Circular Velocity for NGC 4736

To construct a "target" rotation curve for NGC 4736, the data in Figure 20 are normalized. This means that R_m=1 corresponds to 10.38 kpc. Normalizing the velocity (V_m = 125.6 km/s) needs careful treatment to conform with the model. Figure 8 of this paper shows that for a relatively flat rotation curve, the model V_m* equals about 1.24.

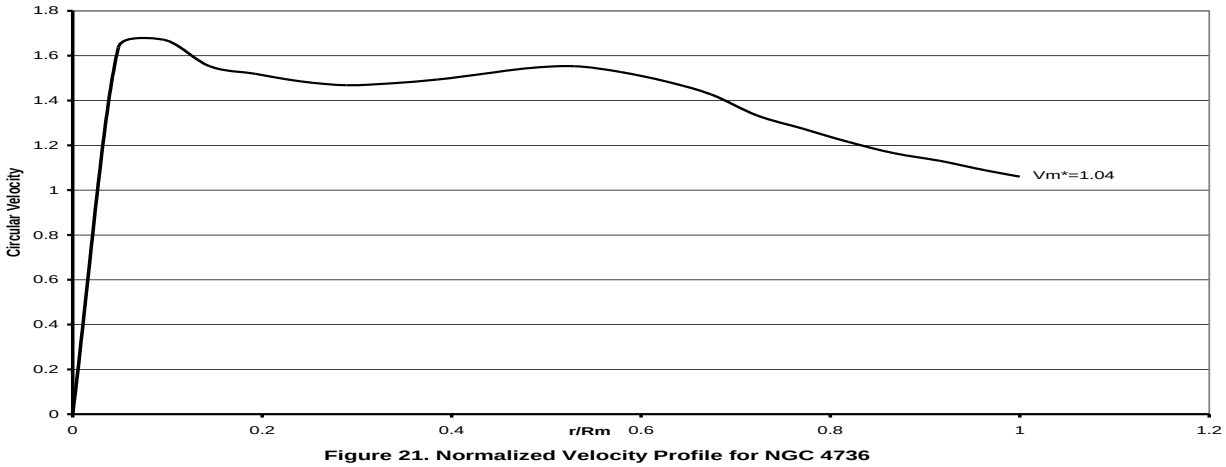

Figure 21. Normalized Velocity Profile for NGC 4736

Experience with various mass distributions has shown the model normalized V_m* can be approximated by

$$V_m^* \approx 0.6\,(V_m/V_{mid}) + 0.63 \qquad (7)$$

where V_{mid} is the velocity of the target rotation curve at about $r/R_m = 0.5$ For NGC 4736, equation 7 suggests an initial model $V_m* \approx 1.04$, and it helps the convergence process to normalize the target rotation curve to reflect this value, as indicated in Figure 21.

A modified L80 mass distribution (see Figure 4.) was chosen as the *starting* model mass distribution for this demonstration. A chart was constructed which compared the velocity (corresponding to the model mass distribution) with the target velocity of Figure 21. The velocity chart (Figure 23) immediately shows the effect of any changes to the model ring mass distribution, so the convergent process becomes interactive.

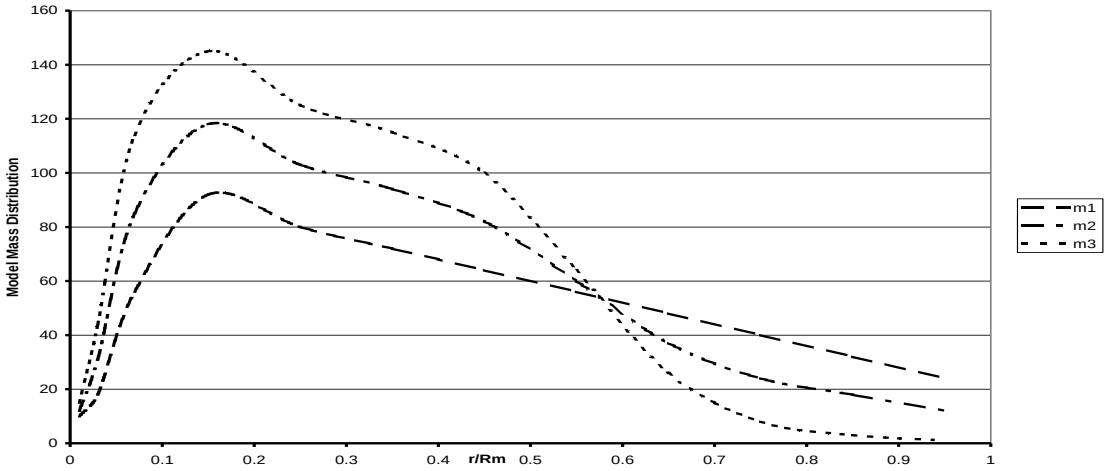

Figure 22. Stages of Model Mass Distribution for NGC 4736

Figure 22 shows the successive stages in the mass distribution adjustment, and Figure 23 shows the corresponding stages in the model velocity profile as it converges with the target profile of NGC 4736. The process consists of changing one or two individual ring mass values and immediately reviewing whether the changes are favorable and leading to convergence.

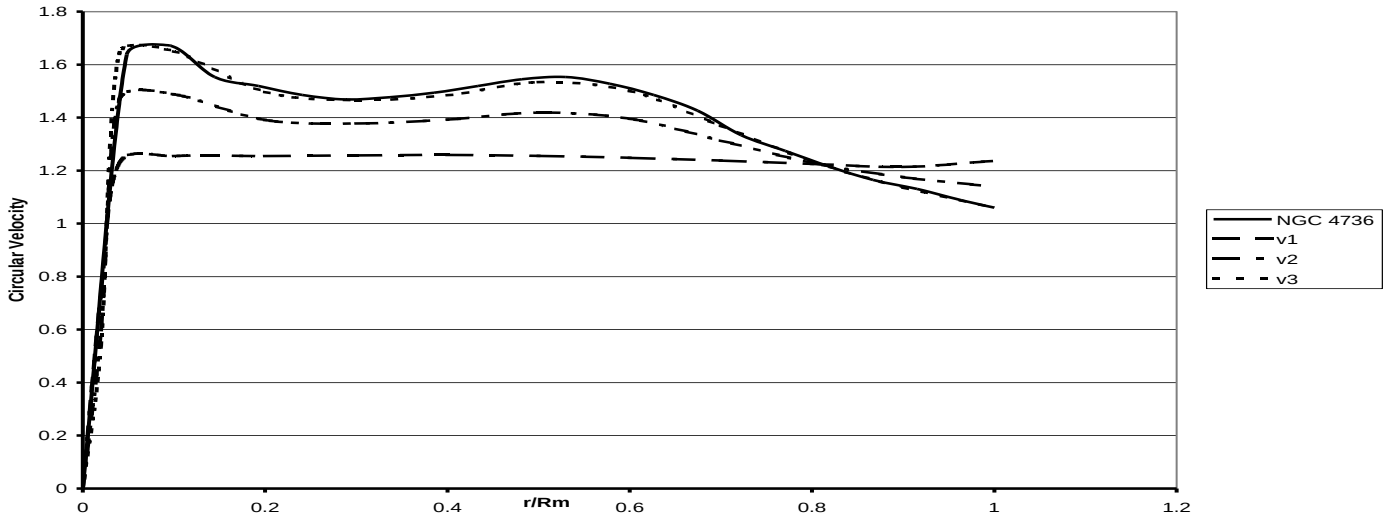

Figure 23. Convergence of Model Velocity to match NGC 4736

Since the model is recognizing mass values both inward and outward from the radial point of interest, the method tends to be counter-intuitive, but becomes manageable with practice. The three stages shown in Figures 22 and 23 involved a total of about 100 individual ring mass adjustments and was completed in about 20 minutes. As the convergent process approaches its final adjustment, the model data indicates that the velocity at $r/R_m = 1$ is settling at $V_m^* = 1.06$, so the target rotation curve is scaled up to reflect this small change. With only 12 discrete mass points, it is obvious that this simplistic match with the target rotation curve will be approximate, but this may be satisfactory for many situations.

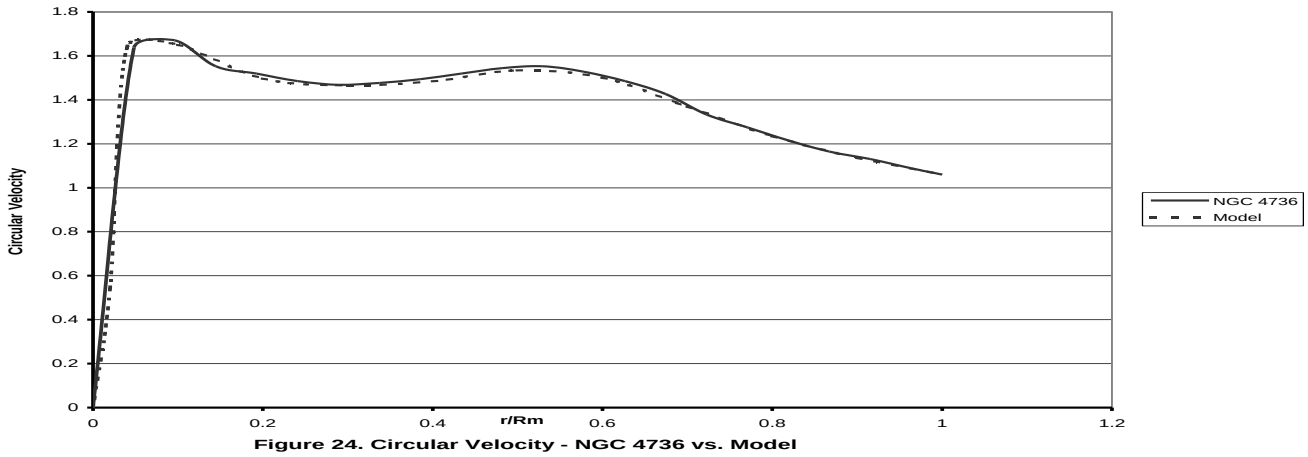

Figure 24. Circular Velocity - NGC 4736 vs. Model

Figure 24 shows the final match between the model velocity profile and NGC 4736 data.

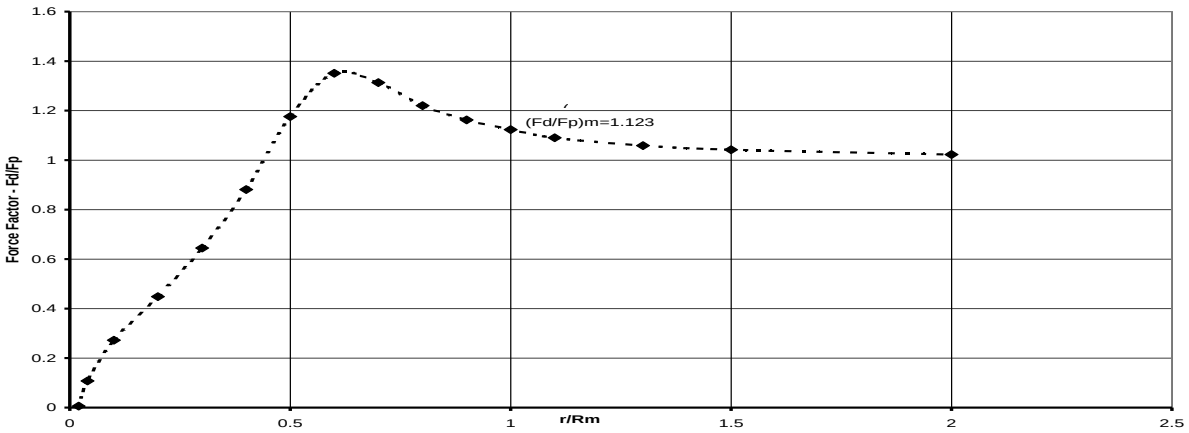

Figure 25. Gravitational Force Factor for NGC 4736 Model

The gravitational force factor (F_d/F_p) in the disk is calculated for the final mass distribution, and is shown in Figure 25. The factor crests with a value of about 1.38 at $r/R_m = 0.6$, and has a value of 1.123 at $r/R_m = 1$.

The relevant data for estimating the galaxy mass of NGC 4736 enclosed within R_m are:

$R_m = 10.38$ kpc $\qquad V_m = 125.6$ km/s $\qquad (F_d/F_p)_m = 1.123$

Mass of NGC 4736 is…. $M_m = 3.39 \times 10^{10} M_\odot$

Figure 26 shows the ring mass distribution that produced the model velocity profile that matched the NGC 4736 rotation curve. Figure 27 translates this ring mass distribution into a Surface Mass Density format. This SMD corresponds closely with that shown in Figure 4 of Reference 5, which was derived by a different methodology, thus providing some validation for the model proposed in this paper.

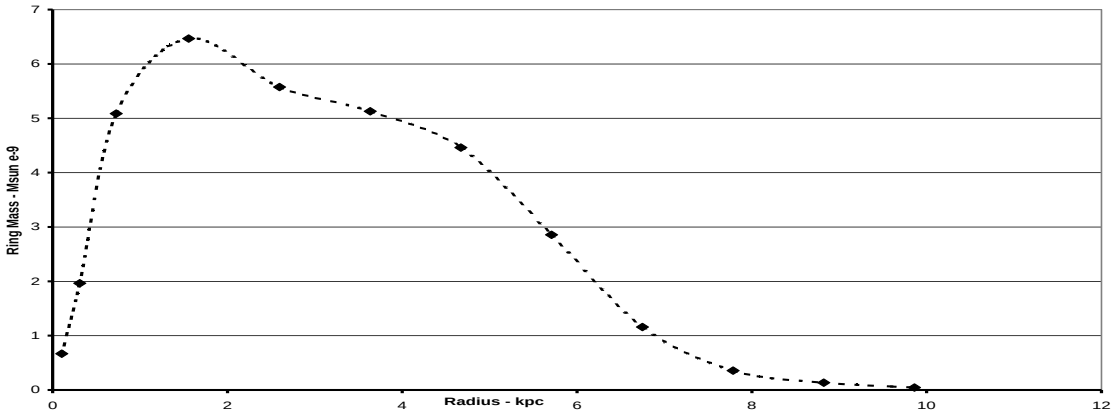

Figure 26. Ring Mass Distribution for NGC 4736 Model

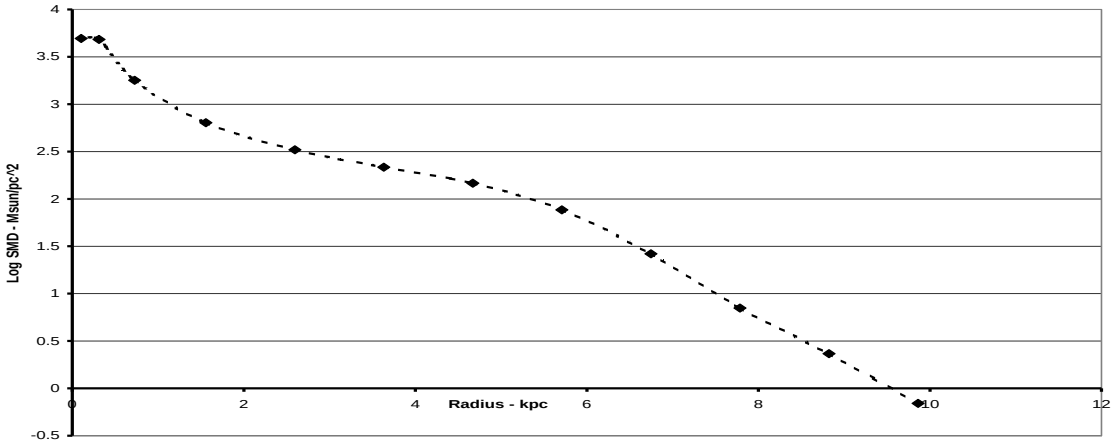

Figure 27. Surface Mass Density for NGC 4736 Model

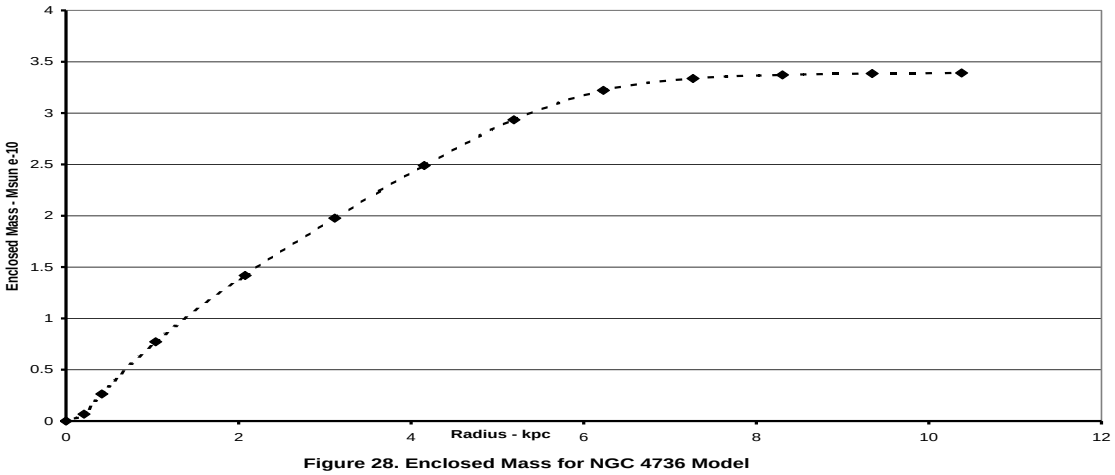

Figure 28. Enclosed Mass for NGC 4736 Model

Figure 28 shows the buildup of the enclosed galaxy mass for the NGC 4736 Model. The enclosed galaxy mass estimate of 3.39 x 10^{10} $M_{\odot}$ is close to the value of 3.43 x 10^{10} $M_{\odot}$ derived by a different methodology in Reference 5.

Appendix 2. Basic characteristics of several Spiral Galaxies

The mass distributions and enclosed galaxy mass for several spiral galaxies (as noted in Table 1 below) have been analyzed using the Model proposed in this paper. In the following pages, three basic charts are provided for each galaxy:

a. A chart showing the published rotation curve data for the galaxy (solid line) and the model matching curve (dashed line).
b. A chart showing the associated ring mass distribution predicted by the model.
c. A chart showing the associated (log) surface mass density distribution.

The objective of this appendix is to demonstrate the capability of the Model in analyzing a selection of spiral galaxies with widely varying rotation curve shapes. Table 1 provides the summary details of the spiral galaxies that have been analyzed in this paper and the appendices.

Galaxy	Type	R_m kpc	V_m km/s	M_m $10^{10}M_\odot$	SMD_{av} $M_\odot/pc^2$	$(F_d/F_p)_m$
Milky Way[12]	**Sb**	**29.3**	**212.0**	**20.9**	**77.5**	**1.46**
M**31**[4]	**Sb**	**34.73**	**226.8**	**28.0**	**73.9**	**1.48**
NGC 598[6]	**Scd**	**15.4**	**136.0**	**3.72**	**49.9**	**1.78**
NGC 2590[13]	**Sbc**	**15.8**	**275.0**	**17.7**	**226.0**	**1.57**
NGC 3031[12]	**Sab**	**21.0**	**169.5**	**10.8**	**78.0**	**1.29**
NGC 3198[2]	**Sc**	**29.7**	**149.0**	**10.0**	**36.2**	**1.53**
NGC 4157[11]	**Sb**	**30.8**	**185**	**16.2**	**54.4**	**1.51**
NGC 4736[5]	**Sab**	**10.38**	**125.6**	**3.39**	**100.1**	**1.12**
NGC 5533[8]	**Sab**	**97.5**	**230.0**	**80.0**	**26.8**	**1.50**
NGC 6744[9]	**Sbc**	**39.2**	**217.0**	**25.1**	**52.0**	**1.71**
NGC 6946[10]	**Scd**	**29.4**	**159.0**	**11.9**	**43.8**	**1.45**
UGC 2885[10]	**Sbc**	**72.6**	**298.0**	**95.6**	**57.7**	**1.57**

The superscripts next to the galaxy designation indicate the Reference which provided the published rotation curve data. The Average Surface Mass Density (SMD_{av}) is the enclosed galaxy mass (M_m) divided by the circular disk area bounded by R_m.

Table 1. Basic characteristics of several Spiral Galaxies

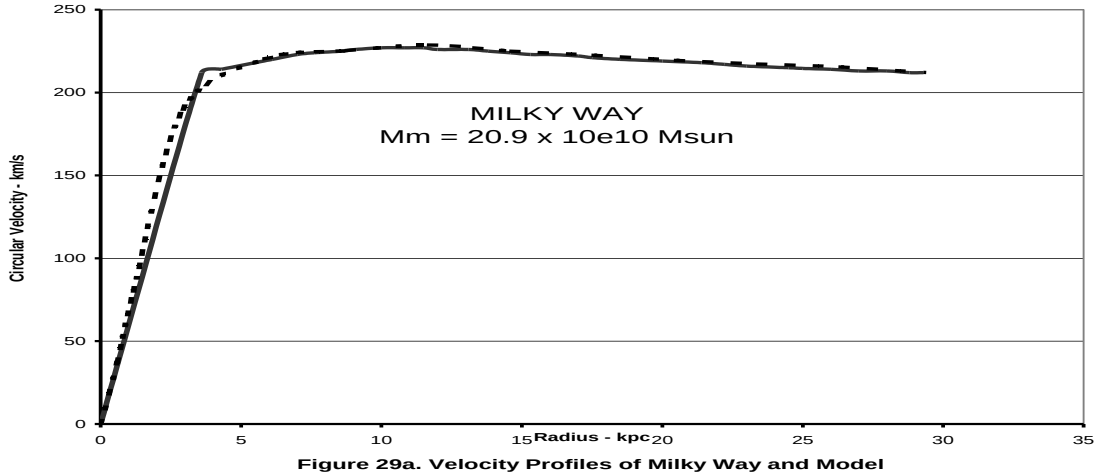

Figure 29a. Velocity Profiles of Milky Way and Model

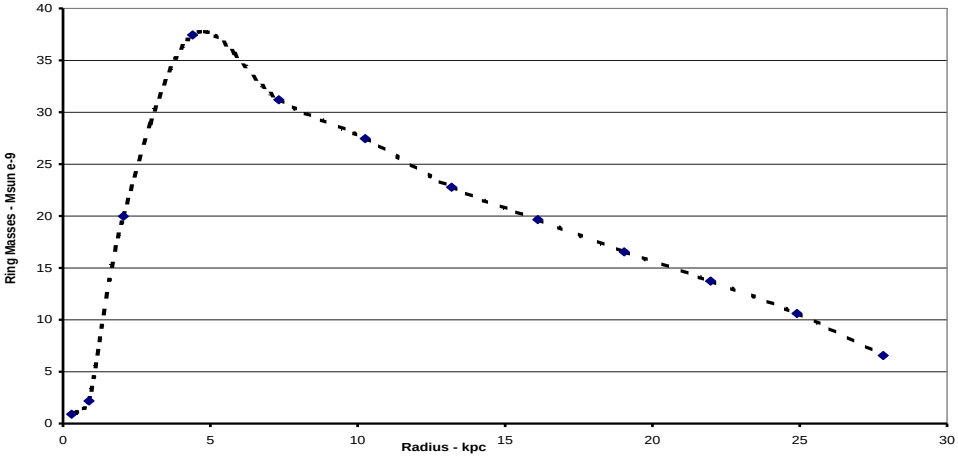

Figure 29b. Ring Mass Distribution for Milky Way Model

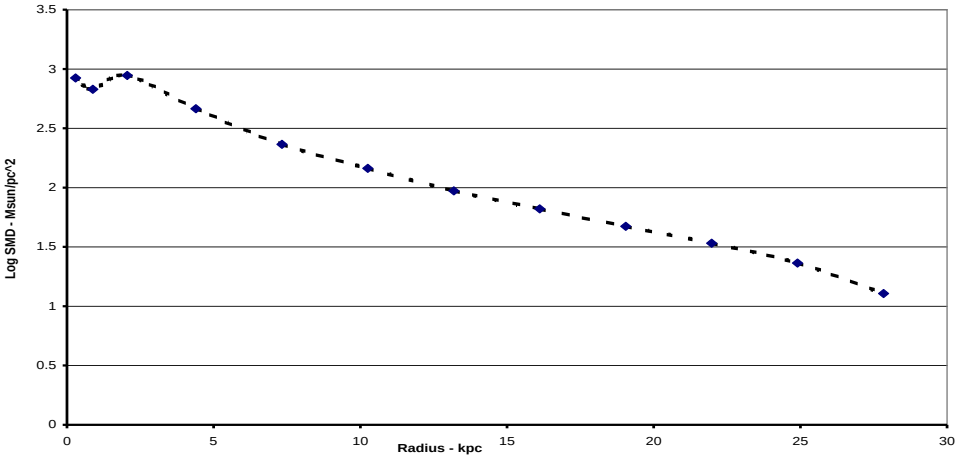

Figure 29c. Surface Mass Density for Milky Way Model

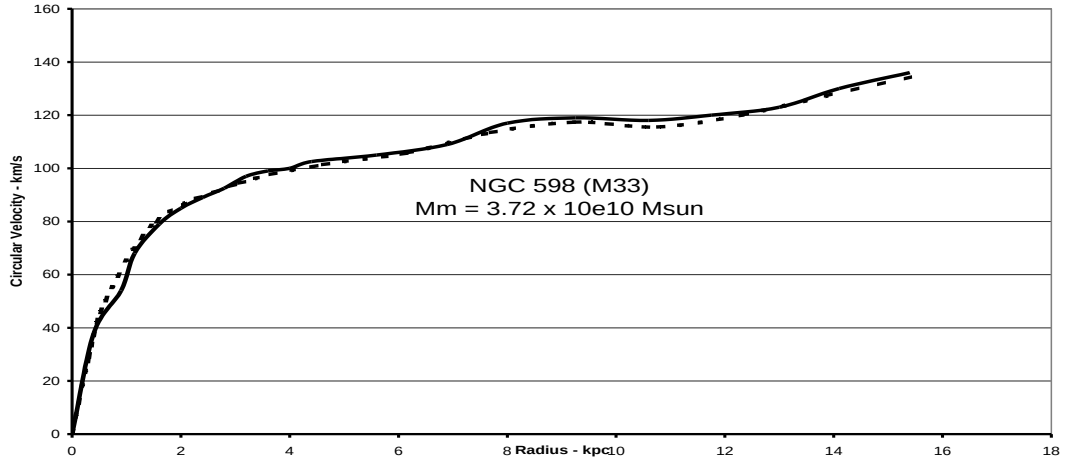

Figure 30a. Velocity Profiles for M33 and Model

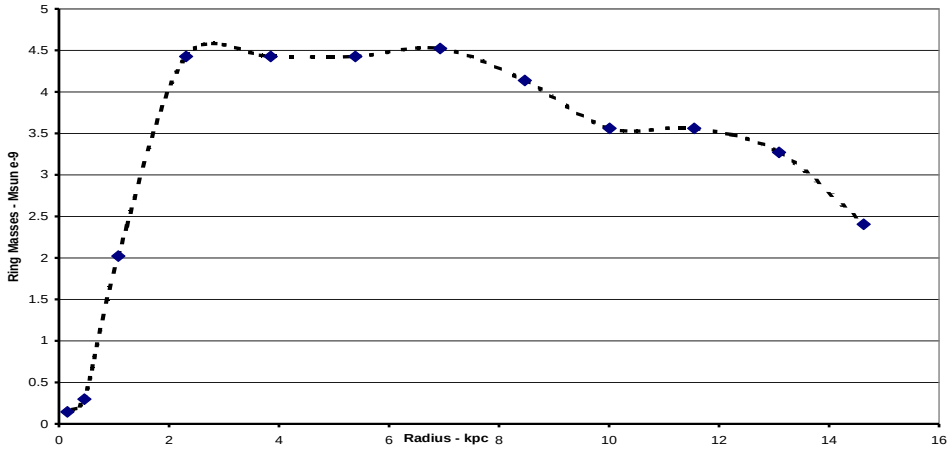

Figure 30b. Ring Mass Distribution for M33 Model

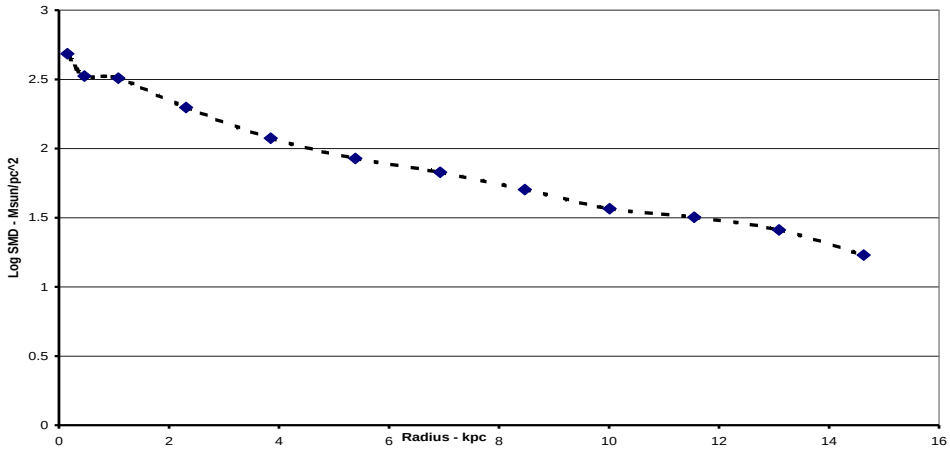

Figure 30c. Surface Mass Density for M33 Model

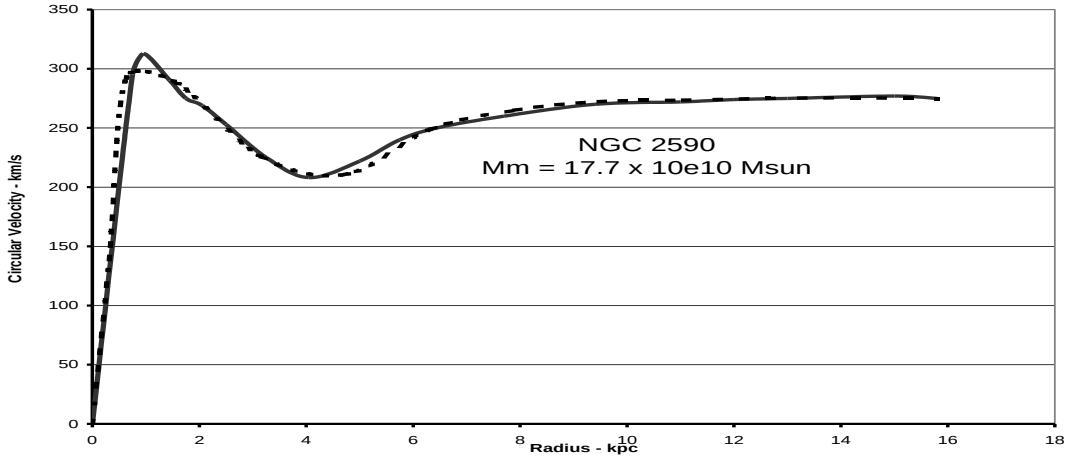

Figure 31a. Velocity Profiles for NGC 2590 and Model

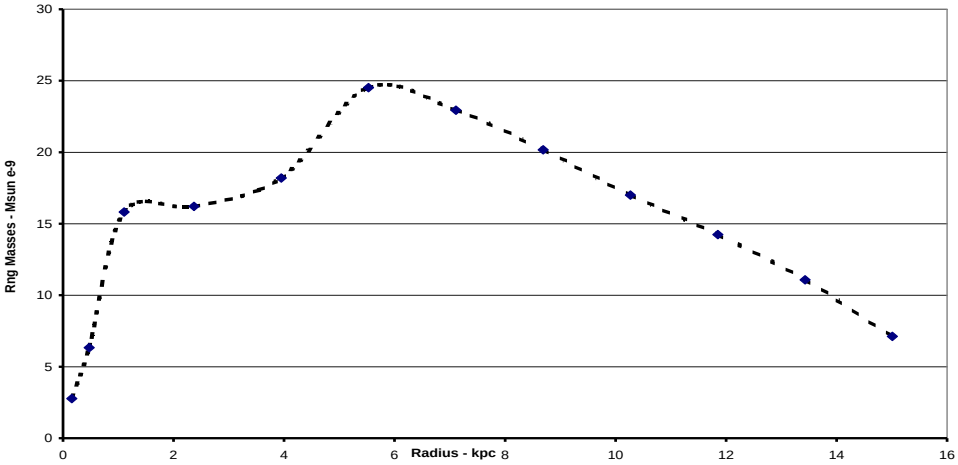

Figure 31b. Ring Mass Distribution for NGC 2590 Model

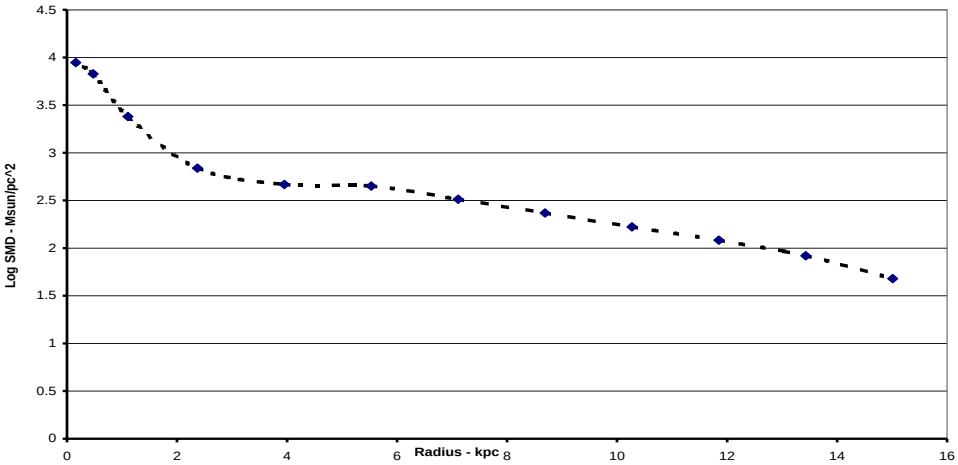

Figure 31c. Surface Mass Density for NGC 2590 Model

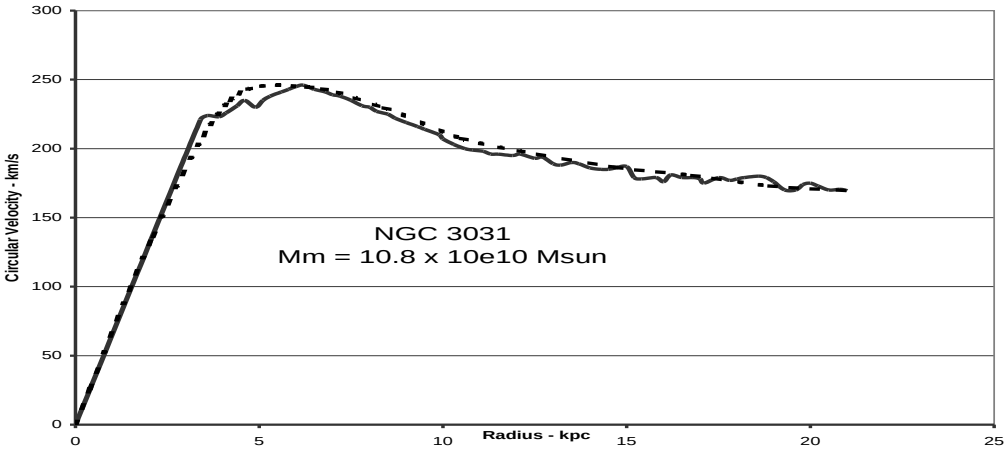

Figure 32a. Velocity Profiles of NGC 3031 and Model

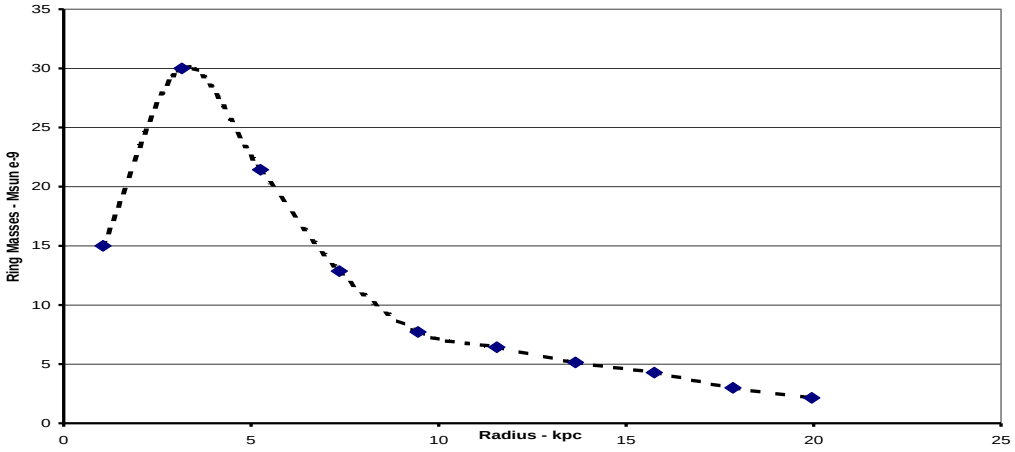

Figure 32b. Ring Mass Distribution for NGC 3031 Model

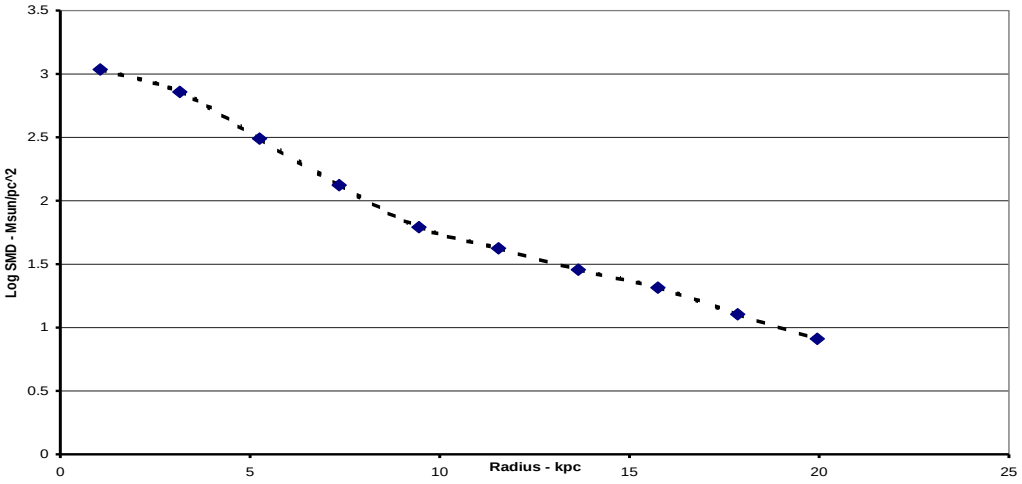

Figure 32c. Surface Mass Density for NGC 3031 Model

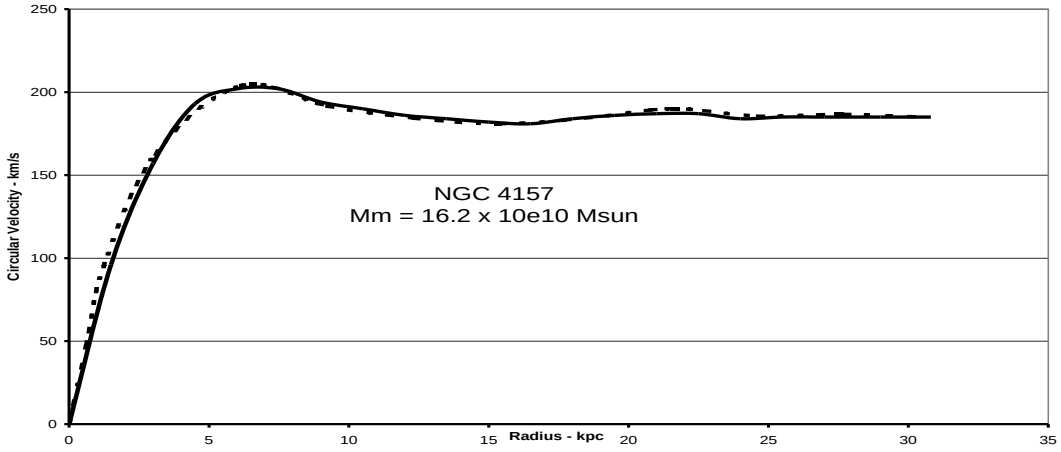

Figure 33a. Velocity Profiles of NGC 4157 and Model

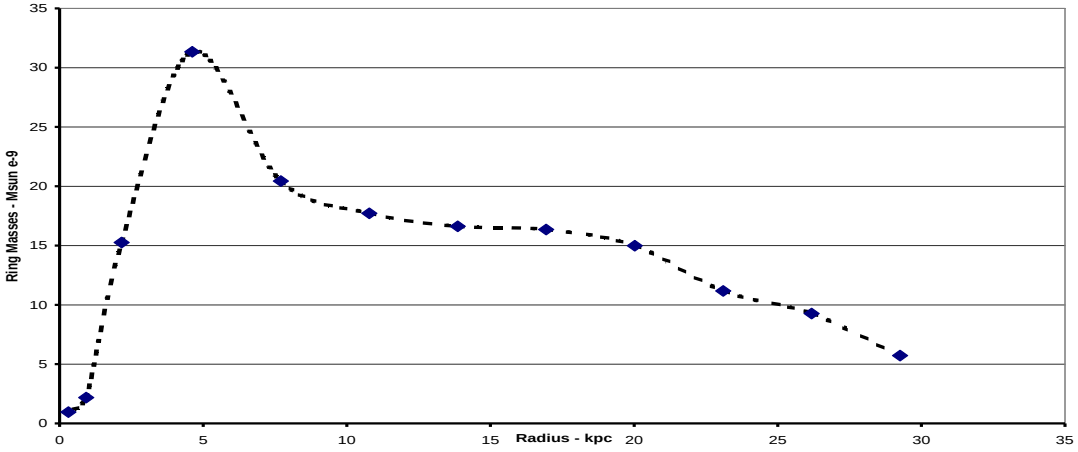

Figure 33b. Ring Mass Distribution for NGC 4157 Model

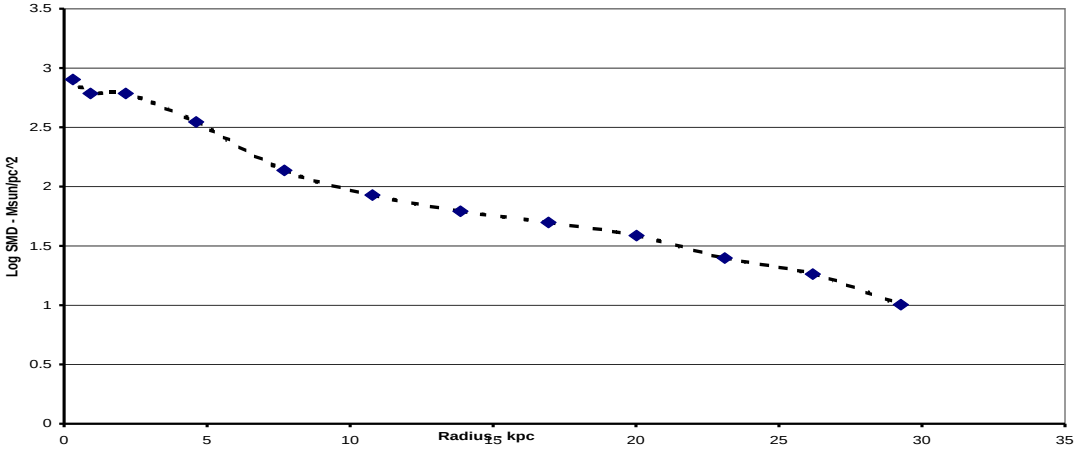

Figure 33c. Surface Mass Density for NGC 4157 Model

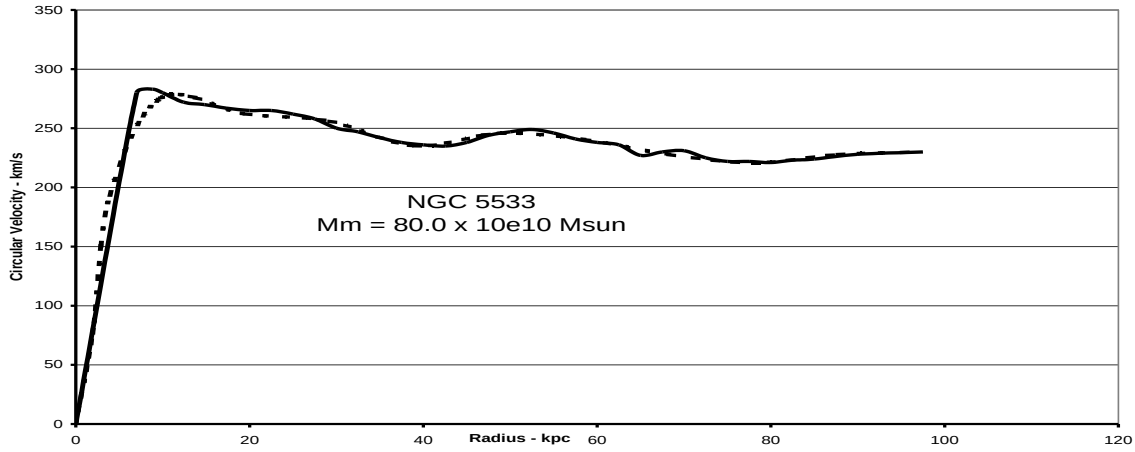

Figure 34a. Velocity Profiles of NGC 5533 and Model

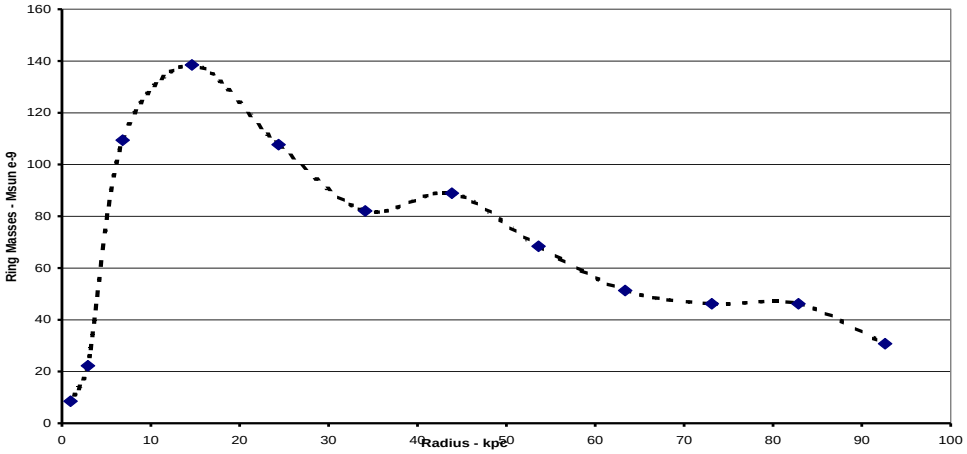

Figure 34b. Ring Mass Distribution for NGC 5533 Model

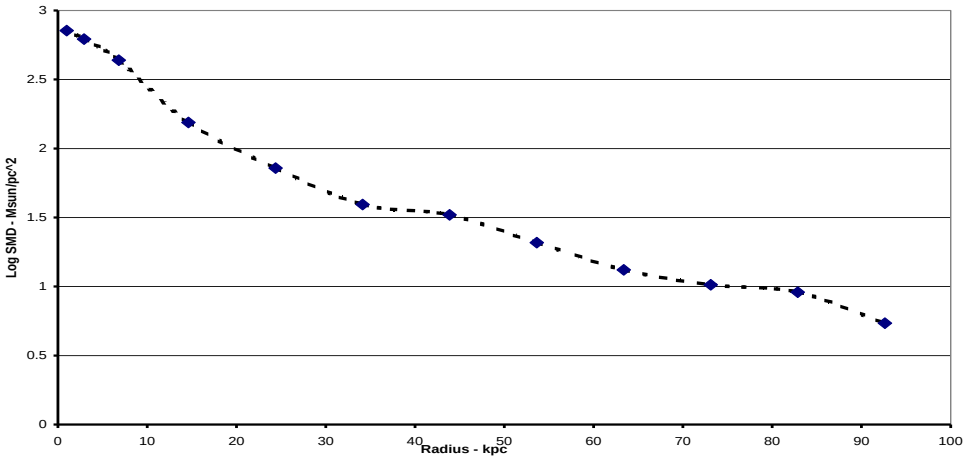

Figure 34c. Surface Mass Density for NGC 5533 Model

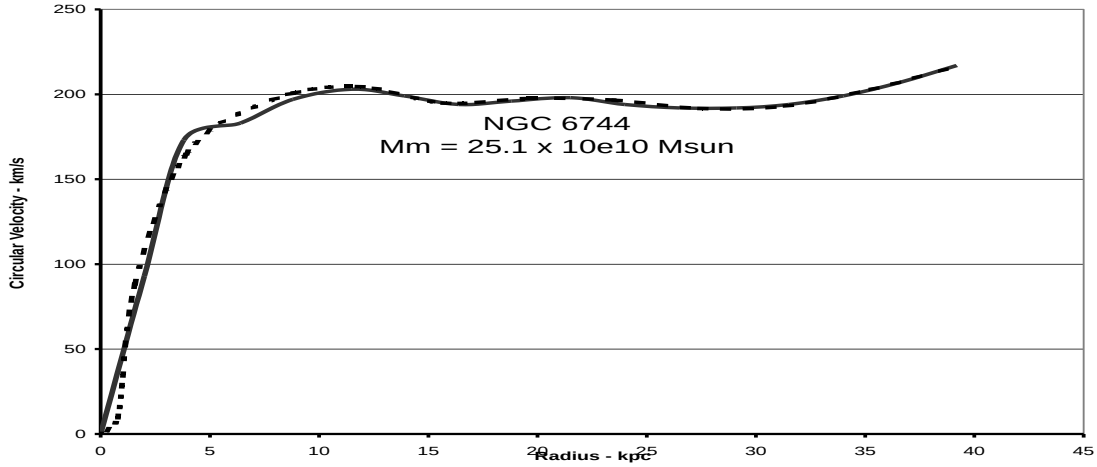

Figure 35a. Velocity Profiles of Milky Way and Model

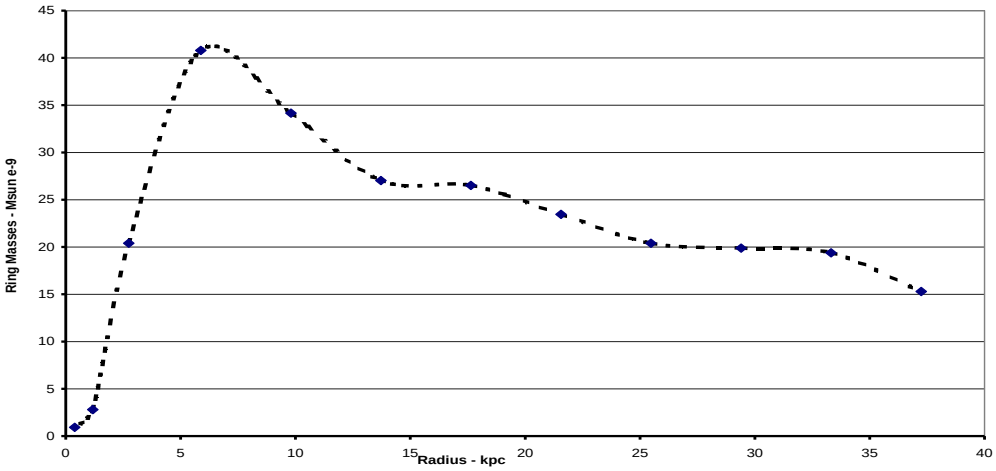

Figure 35b. Ring Mass Distribution for NGC 6744 Model

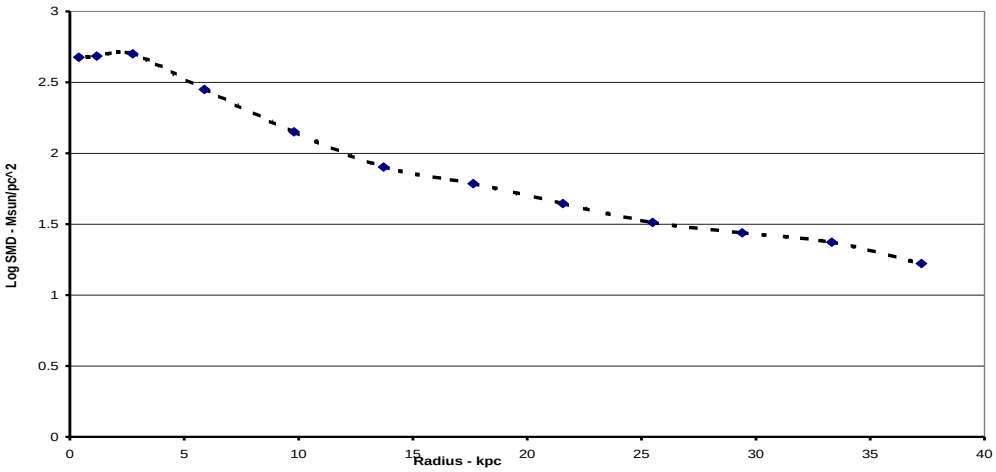

Figure 35c. Surface Mass Density for NGC 6744 Model

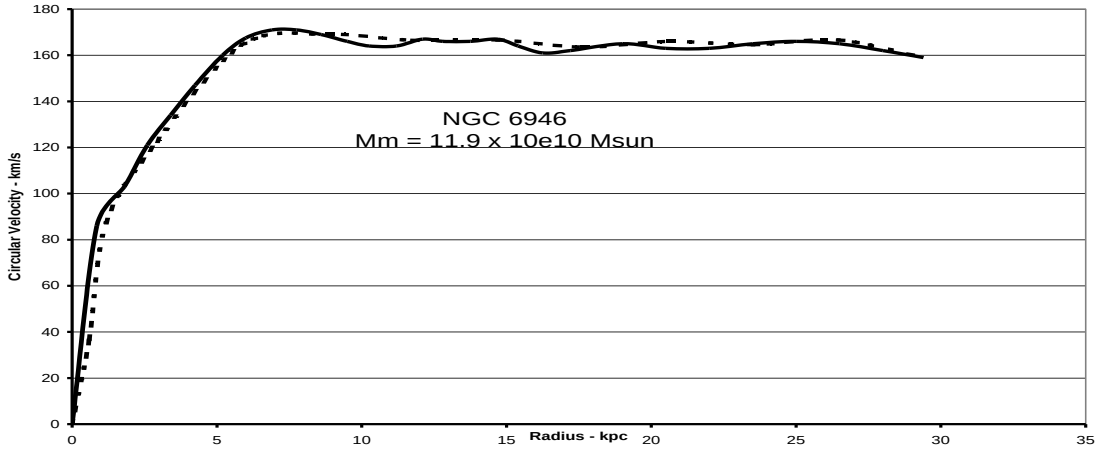

Figure 36a. Velocity Profiles of NGC 6946 and Model

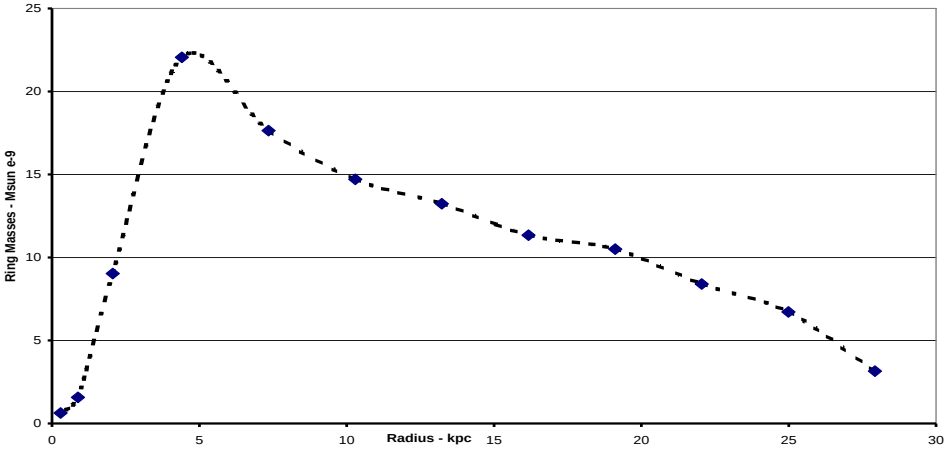

Figure 36b. Ring Mass Distribution for NGC 6946 Model

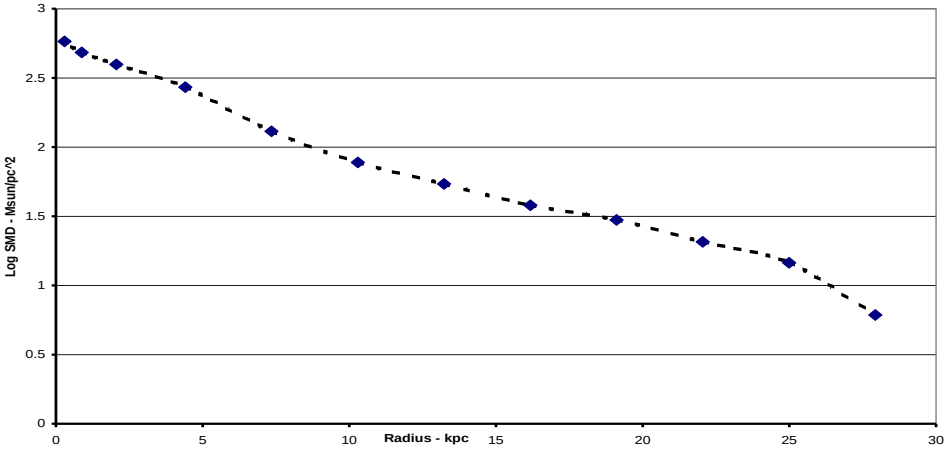

Figure 36c. Surface Mass Density for NGC 6946 Model

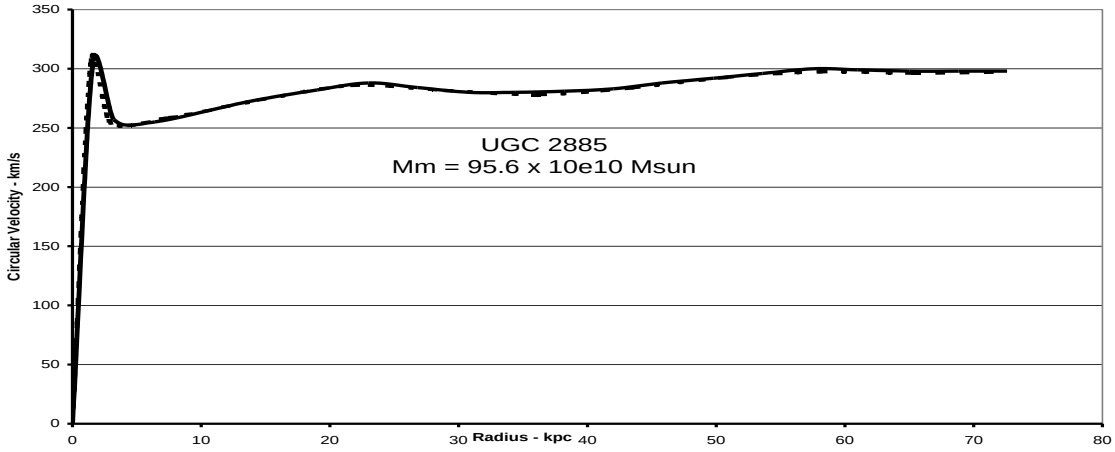

Figure 37a. Velocity Profiles of UGC 2885 and Model

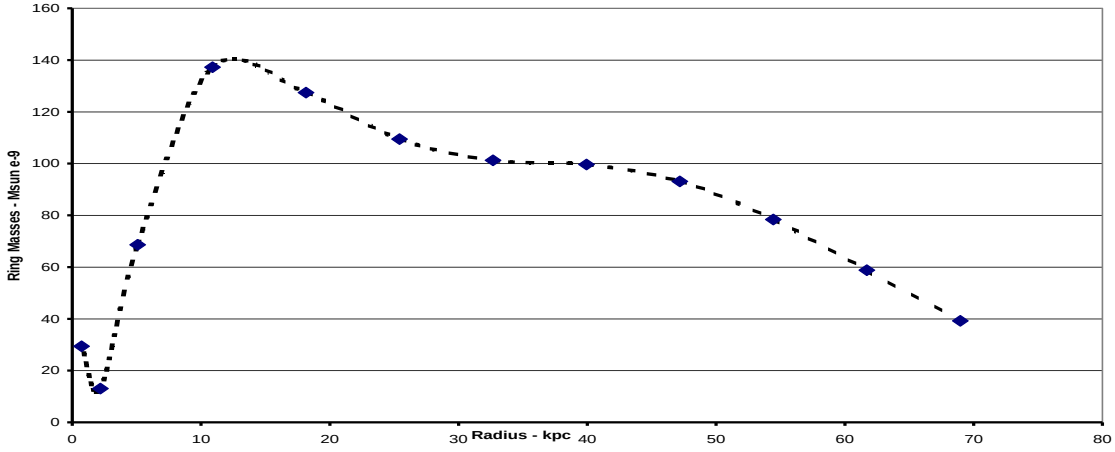

Figure 37b. Ring Mass Distribution for UGC 2885 Model

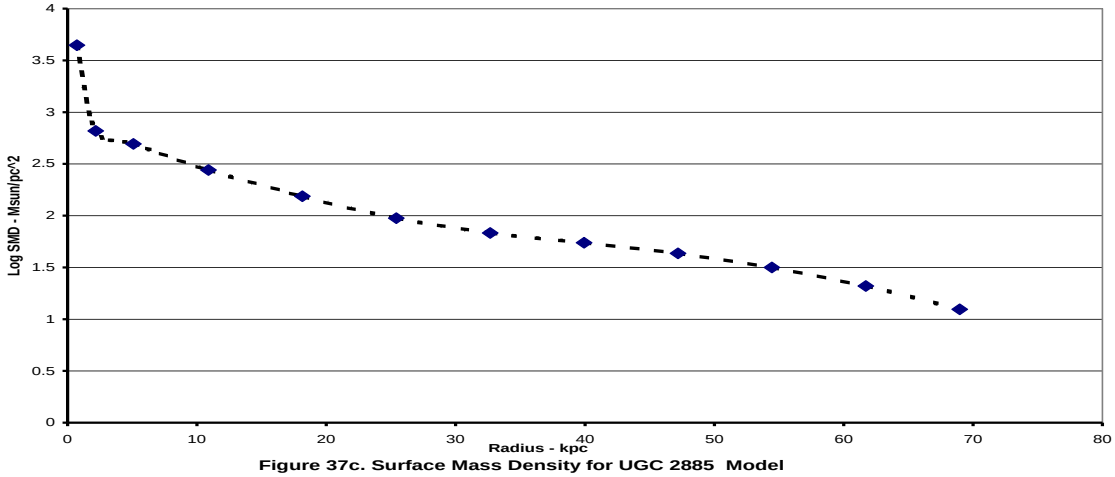

Figure 37c. Surface Mass Density for UGC 2885 Model